AD 270 827

UNCLASSIFIED

AFCRL 989

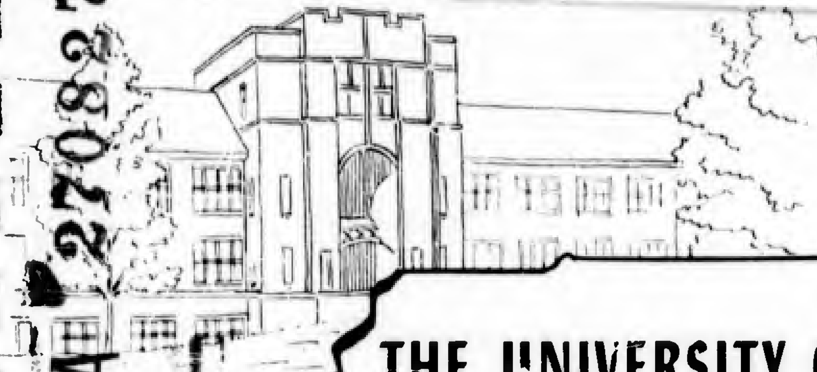

THE UNIVERSITY OF TENNESSEE

DEPARTMENT OF ELECTRICAL ENGINEERING

ELECTRONIC SCANNING OF CIRCULAR ANTENNA ARRAYS

by

H. P. Neff, D. R. Stephens, and J. D. Tillman

Scientific Report No. 5
1 December 1961

Air Force Cambridge Research Laboratories
Contract AF 19(604)-4967

A PROJECT OF THE ENGINEERING EXPERIMENT STATION
THE UNIVERSITY OF TENNESSEE COLLEGE OF ENGINEERING
Knoxville, Tennessee

Requests for additional copies by Agencies of the Department of Defense, their contractors, and other Goverment agencies should be directed to the:

ARMED SERVICES TECHNICAL INFORMATION AGENCY
ARLINGTON HALL STATION
ARLINGTON 12, VIRGINIA

Department of Defense contractors must be established for ASTIA services or have their 'need-to-know' certified by the cognizant military agency of their project or contract.

All other persons and organizations should apply to the:

U. S. DEPARTMENT OF COMMERCE
OFFICE OF TECHNICAL SERVICES
WASHINGTON 25, D. C.

ARCRL 989

ELECTRONIC SCANNING OF CIRCULAR ANTENNA ARRAYS

by

H. P. Neff, D. R. Stephens, and J. D. Tillman

Scientific Report No. 5
Contract AF 19(604) - 4967

ELECTRICAL ENGINEERING DEPARTMENT
THE UNIVERSITY OF TENNESSEE
KNOXVILLE, TENNESSEE

The research reported in this document has been sponsored by the Electronics Research Directorate of the Air Force Cambridge Research Laboratories, Office of Aerospace Research (USAF) L. G. Hanscom Field, Bedford, Mass. The publication of this document does not constitute approval by the Air Force of the findings or conclusions contained herein.

Air Force Cambridge Research Laboratories
1 December 1961

TABLE OF CONTENTS

LIST OF FIGURES

LIST OF TABLES

ABSTRACT

This report describes an antenna array which consists of concentric rings of monopoles. In each ring all of the elements are fed from two amplifiers, the output of which is controlled by a steady or slowly varying voltage. The antenna forms a directional beam, and the pointing of this beam is determined by the control voltages. The pointing can be continuously varied through 360° without significantly changing the shape of the pattern.

The fundamental theory on which the antenna is based is summarized, and details of the design are presented. The electronic equipment required to give a uniformly rotating beam is described, and the results of stability tests are given. In the last part, the results of a series of tests on such an antenna are described. The antenna which was tested had a beamwidth of about 50°, a side-lobe level of 20 db, and the beam was rotated at steady rate of 60 revolutions per second.

The antenna offers the following advantages:

1. Any angle of pointing can be obtained.
2. The required voltages are easy to generate.
3. Only relatively standard electronic components are required.

I. INTRODUCTION

This report describes a circular antenna array, consisting of concentric rings of monopoles, which forms a directional radiation pattern having low side lobes. Each ring is excited by two amplifiers, and by varying control voltages to these amplifiers the beam may be pointed to any desired azimuth angle.

Circular antenna arrays have been studied intermittently for at least thirty years. Stenzel[1] proposed that a circular array be used in a direction finding system, and gave an analysis of a single-ring array having uniform co-phasal excitation. In his analysis he assumed that the number of elements was even. This analysis was extended by Knudsen[2] to include the case of an odd number of elements. DuHamel[3] developed a synthesis technique by which a specified pattern could be obtained, and also showed how patterns of the Tchebyscheff type can be formed with a circular array. None of these studies were concerned with current distribution along the elements of the array or with the terminal impedance of the elements, or indeed, with whether the required current distribution around the ring could be physically realized. King[4] showed how the integral equation method for studying these properties could be applied to circular arrays and Hickman, Neff and Tillman[5] carried out a detailed analysis of single-ring arrays, which is given in complete form in Scientific Report No. 4 on this contract.

A recent trend in directional antenna arrays is to excite each element of the array from a separate radio-frequency amplifier. The beam can then be pointed in various directions by varying either the phase or the amplitude (or both) of the exciting voltage to this amplifier. This method, called electronic scanning, has been used with linear arrays, but the beam can be pointed only to angles lying within about sixty degrees of the normal to the line of the array. By using such a technique with a circular array, there is obviously no such limitation on scan angle, since any angle is equivalent to any other because of the circular symmetry. A serious difficulty with impedance arises, however, which is not a significant factor with linear arrays. If a single-ring circular array is designed by either the method of DuHammel, or by the related method of Hickman, Neff and Tillman, it is found that the impedance of the various elements varies widely from element to element, and indeed, will sometimes have a negative real part. Thus, since scanning a circular array is equivalent to moving the current distribution around the array, the load impedance on each amplifier varies drastically with scan angle, resulting in poor performance by the amplifier. An additional practical problem is present, since the required amplitude and phase of the amplifier output does not vary in any simple manner, requiring an elaborately programmed control system.

As a result of a study by Neff, Patton, Pierce, and Tillman[6,7] under Contract AF 19(604)-1557, it was found that a pattern of the form cos $k(\phi-\phi_o)$ can be radiated by a single ring, and that all of the elements will have the same impedance. They proposed stacking a number of such rings vertically, each with a different value of k, to give a pattern $\sum \cos k(\phi-\phi_o)$. The vertical stacking results in little coupling between rings, with a consequent steady load on the amplifiers. One purpose of the present contract was to build and test such an antenna. It was found early in the work that under some conditions coupling between rings can be tolerated, and the array actually tested consists of concentric rings of monopoles, with their terminals lying on a common ground plane. Only two amplifiers per ring are needed, and the required control system is relatively simple.

This report describes this antenna, and gives the pertinent design information for both the antenna and the electronic equipment, and the results of a number of tests. Arrays having a center element, and either two and three rings were tested, giving beamwidths of 80^o and 50^o respectively. Side-lobe levels of 20 db to 30 db were easily obtained. The scanning system was designed to rotate the beam at a uniform rate of 60 revolutions per second. Section II gives a summary of the basic theory of circular arrays, and shows the application to the system described above. Section III covers the design of the electronic equipment needed to excite and scan the array, and Section IV gives the results of the tests of the array.

II. THEORY AND DESIGN OF THE ANTENNA

It is the purpose of this section to set down in concise form those results from previous analysis of circular arrays which are needed in the design of a concentric ring scanned array, and to complete such a design. Since the fundamental theory of such arrays is now available in the literature[5,8,9], it will not be repeated here.

A. Isolated Ring with Sequence Excitation.

Consider a circular array with a radius ρ_1 consisting of m identical parallel monopoles, as shown in Fig. II-1. The elements are numbered from 1 to m, and the center of element m lies in the plane $\phi = 0$ of a spherical coordinate system whose center lies at the center of the ring. The centers of all of the elements lie in the plane $\theta = \pi/2$, and all of the elements are perpendicular to this plane. Let the current in the i^{th} element be

$$I_i^{(k)} = I^{(k)} \cos\left(\frac{2\pi}{m} ki - k\phi_o\right). \tag{1}$$

In (1), k is any positive integer and is called the sequence number, $I^{(k)}$ is a complex constant called the sequence current, and ϕ_o is any fixed angle. The time variation $e^{j\omega t}$ is understood. The far field pattern of this set of currents is[6]

$$F^{(k)}(\theta,\phi) = m\, I^{(k)} \Bigg\{ j^k J_k(\beta\rho \sin\theta)\cos k(\phi-\phi_o) + \sum_{p=1}^{\infty} \Big[j^{(pm-k)} J_{pm-k}(\beta\rho\sin\theta)\cos(pm\phi - k\phi + k\phi_o) + j^{(pm+k)} J_{pm+k}(\beta\rho\sin\theta)\cos(pm\phi + k\phi - k\phi_o)\Big]\Bigg\}. \tag{2}$$

The element factor, $F_e(\theta)$ is omitted from (2). $J_n(x)$ is the n^{th} order Bessel function of the first kind, and β is the phase constant $2\pi/\lambda$. Inspection of (2) shows that if $\beta\rho$ k, and m-k >>k, then all of the terms in the summation are neglible. It is accordingly convenient to call the term outside of the summation the principle term, and the remaining terms residuals. These may be made as small as desired by making m large. If m is so chosen,

$$F^{(k)}(\theta,\phi) = j^k\, m\, I^{(k)}\, J_k(\beta\rho \sin\theta) \cos k(\phi-\phi_o). \tag{3}$$

Inspection of (1) shows that if m is even, there are only m/2 choices of k that lead to different sets of currents. If m is odd, there are (m+1)/2 choices of k. Equation (1) can be written

$$I_i = I^{(k)} \left(\cos \frac{2\pi ki}{m} \cos k\phi_o + \sin \frac{2\pi ki}{m} \sin k\phi_o\right). \tag{4}$$

If we now set m = 4, $2\pi ki/m = \pi i/2$, and

$$I_i = I^{(k)} \left(\cos \frac{\pi}{2}\, i \cos k\,\phi_o + \sin \frac{\pi}{2}\, i \cos k\,\phi_o\right). \tag{5}$$

For i odd, $\cos \frac{\pi}{2}\, i = 0$, and for i even, $\sin \frac{\pi}{2}\, i = 0$. Then

$$\begin{aligned} I_i &= j^{(i-1)}\, I^{(k)} \sin k\,\phi_o, && \text{(i odd)}, \\ &= j^i\, I^{(k)} \cos k\,\phi_o, && \text{(i even)}. \end{aligned} \tag{6}$$

Let $\beta\rho = k$. Then the principal term is

$$F^{(k)}(\theta,\phi) = j^k\, 4k\, I^{(k)}\, J_k(k \sin\theta) \cos k(\phi-\phi_o), \tag{7}$$

and the largest residual is

$$F_R^{(k)}(\theta,\phi) = j^{3k}\, 4k\, I^{(k)}\, J_{3k}(k \sin\theta) \cos(3k\phi + k\phi_o), \tag{8}$$

which is always small compared to the principal term.

It is now evident that if currents as specified by (6) can be maintained, an array of concentric rings may be constructed with values of k = 1, 2, --- K. The inner ring will have 4 elements, the next ring 8, the third ring 12, and the K^{th} ring will have 4K elements. The pattern will be

$$F(\theta,\phi) = \sum_{k=1}^{K} j^k \, 4k \, I^{(k)} J_k(k \sin \theta) \cos k(\phi - \phi_o). \tag{9}$$

Since the Fourier series of a directional pattern requires a constant term, this can be provided by adding an element at the center with current $I^{(o)}$.

$$\text{Let } A_k = j^k \, 4k \, I^{(k)} J_k(z), \qquad k \neq 0,$$
$$= I^{(o)}, \qquad k = 0. \tag{10}$$

Then at $\theta = \pi/2$,

$$F\left(\frac{\pi}{2}, \phi\right) = \sum_{k=0}^{K} A_k \cos k(\phi - \phi_o). \tag{11}$$

The constants A_k may be chosen as desired to give a satisfactory pattern. It is clear that the beam is pointed to the angle ϕ_o.

Referring to (6) it is seen that all of the currents in any one ring are in phase with each other, and that they have amplitudes of either $\pm I^{(k)} \sin k\phi_o$ or $\pm I^{(k)} \cos k\phi_o$. If these currents are supplied from controlled amplifiers, only two amplifiers per ring are needed. If all of the A_k's in (11) are real, as is usual in pattern synthesis, (10) indicates there is a phase lag 90° in the phases of successive $I^{(k)}$'s. The properties of each ring of such an array of concentric rings are summarized in Table II-1.

Table II-1

Required currents and resulting patterns of single-ring arrays for sequence excitation, $m = 4k$, $\beta\rho = k$.

k	m	Currents i odd	Currents i even	$I^{(k)}$	Pattern
0	1	-	$I^{(o)}$	A_o	A_o
1	4	$I^{(1)}\sin\phi_o$	$I^{(1)}\cos\phi_o$	$-jA_1/4J_1(1)$	$A_1\cos(\phi-\phi_o)$
2	8	$I^{(2)}\cos2\phi_o$	$I^{(2)}\cos2\phi_o$	$-A_2/8J_2(2)$	$A_2\cos2(\phi-\phi_o)$
3	12	$I^{(3)}\sin3\phi_o$	$I^{(3)}\cos3\phi_o$	$jA_3/12J_3(3)$	$A_3\cos3(\phi-\phi_o)$
4	16	$I^{(4)}\sin4\phi_o$	$I^{(4)}\cos4\phi_o$	$A_4/16J_4(4)$	$A_4\cos4(\phi-\phi_o)$

If a single ring array has currents, given by (1) all of the elements will have the same terminal impedance, called the sequence impedance. This impedance, for the case of $h = \lambda/4$, is

$$Z^{(k)} = j\,\frac{\eta}{4\pi}\sum_{i=1}^{m} e^{\frac{2\pi ki}{m}}\, C_d\left(\frac{\lambda}{4}, \frac{\lambda}{4}\right) \tag{12}$$

In (12), $Z^{(k)}$ is the sequence impedance, η is intrinsic impedance of free space ($\eta = 120\pi$), and

$$C_d\left(\frac{\lambda}{4}, \frac{\lambda}{4}\right) = \int_{-\lambda/4}^{\lambda/4} \frac{\cos\beta\bar{z}\; e^{-j\beta R_{mi}}\, d\bar{z}}{R_{mi}}\ , \tag{13}$$

where $R_{mi} = d_{mi} + \left(\frac{\lambda}{4} - \bar{z}\right)^2$, and d_{mi} is the spacing between the m^{th} element and the i^{th} element. The function $C_d(h,z)$ has been tabulated by Mack and Mack[10]. Extensive tables of $Z^{(k)}$ are to be found in Scientific Report No. 4 on this contract. Table II-2 gives values pertinent to the case considered here.

Table II-2

Sequence Impedances for single-ring arrays for the case of $m = 4k$, $\beta\rho = k$.

k	$R^{(k)}$	$X^{(k)}$
1	48.2	78.4
2	56.2	102.0
3	60.3	117.6
4	62.9	129.3

Unfortunately, if either a center element, or more than one ring is present, coupling between rings is such that the impedances of all of the elements are no longer the same. This coupling between rings is considered next.

B. Coupling Between Concentric Rings.

It has been shown that if the currents in the k^{th} ring are of the form

$$I_i^{(k)} = I^{(k)} \cos(\pi i - k\phi_o), \tag{1}$$

the pattern will be

$$F^{(k)} = j^k \, 4k \, I^{(k)} J_k(\beta\rho \sin\theta) \cos k(\phi - \phi_o). \tag{2}$$

If there were no other rings present, the impedance of each element is the same, $Z^{(k)}$. Then the required voltage at the terminal of each element would be simply

$$V_i^{(k)} = I_i^{(k)} Z^{(k)} = I^{(k)} Z^{(k)} \cos(\pi i - k\phi_o). \tag{3}$$

As soon as there are currents in the other rings (3) no longer holds because of mutual coupling, and the set of voltages required to give the current set $I_i^{(k)}$ becomes very complicated. Suppose however, each ring is excited with voltages of the form of (3), and it is now desired to find the resulting pattern. This pattern can be found by superposition of the patterns when each ring alone is driven by the voltage set (3), with all of the elements in other rings terminated in the generator internal impedances. To find these patterns requires the determination of the currents induced in the undriven rings.

First, consider only one ring, driven by a set of voltages specified by (3), and a center element terminated in Z_g. Since each element in the ring is equidistant from the center element, and the sum of the currents is zero, the induced current in the center element is zero, and driving the ring gives the same result as if the center element were not present. If the center element is driven, and the elements in the ring are terminated in Z_g, equal currents will be induced in each element of the ring. The pattern obtained by driving the center element is thus

$$F^{(o)} = I_o + 4k\, I_o'\, J_o\, (\beta\rho \sin\theta), \tag{4}$$

in which I_o' is the current induced in each element in the ring. To find this current, consider the coupled circuit equations for this case:

$$V_o = I_o Z_{11} + \sum_{i=1}^{4k} I_o' Z_\rho ,$$

$$-I_o' Z_g = I_o Z_\rho + I_o' (Z_{11} + Z_{12} + \cdots Z_{1\,4k}) . \tag{5}$$

Z_ρ is the mutual impedance between the center element and each element in the ring, and the sum in the brackets can be recognized as the zero-sequence impedance of the ring. From (5)

$$I_o' = -I_o \frac{Z_\rho}{Z^{(o)}+Z_g} , \tag{6}$$

$$\frac{V_o}{I_o} = Z_{11} - \frac{4kZ_\rho^2}{Z^{(o)}+Z_g} = Z_o. \tag{7}$$

Now if both the ring and center element are driven, by superposition,

$$I_o = \frac{V_o}{Z_o} ,$$

and

$$I_i = I_o' + \frac{V_i^{(k)}}{Z^{(k)}} .$$

The pattern is consequently

$$F = \frac{V_o}{Z_o} \left[1 - \frac{Z_\rho}{Z^{(o)} + Z_g} \; J_o (\beta\rho \sin\theta) \right]$$

$$+ \frac{V^{(k)}}{Z^{(k)}} \; j^k \, 4k \, J_k (\beta\rho \sin\theta) \cos k (\phi - \phi_o). \qquad (8)$$

It is seen that (8) gives precisely the desired pattern: a constant term which depends only on the voltage V_o applied to the center element, and a term $\cos k (\phi-\phi_o)$ which depends on the voltage $V^{(k)}$.

Consider next two concentric rings, each having four elements, with the elements not necessarily lying on the same radial. Let the elements be numbered as shown in Fig. II-2, which also shows the nomenclature used for the mutual impedances. That is, ${}_{IJ}Z_{ij}$ is the mutual impedance between element i in the I^{th} ring, and element j in the J^{th} ring. The circuit equations for this eight element array are

$${}_{1}V_{4} = {}_{1}I_{4}\,{}_{11}Z_{44} + {}_{1}I_{1}\,{}_{11}Z_{41} + {}_{1}I_{2}\,{}_{11}Z_{42} + {}_{1}I_{3}\,{}_{11}Z_{43}$$

$$+ {}_{2}I_{4}\,{}_{12}Z_{44} + {}_{2}I_{1}\,{}_{12}Z_{41} + {}_{2}I_{2}\,{}_{12}Z_{42} + {}_{2}I_{3}\,{}_{12}Z_{43} ,$$

$$ {}_1V_1 = {}_1I_4 Z_{11\,14} + {}_1I_1 Z_{11\,11} + {}_1I_2 Z_{11\,12} + {}_1I_3 Z_{11\,13} \,, \qquad (9)$$

$$ + {}_2I_4 Z_{12\,14} + {}_2I_1 Z_{12\,11} + {}_2I_2 Z_{12\,12} + {}_2I_3 Z_{12\,13} \,, $$

$$ {}_2V_3 = {}_1I_4 Z_{12\,43} + {}_1I_1 Z_{12\,13} + {}_1I_2 Z_{12\,23} + {}_1I_3 Z_{12\,33} $$

$$ + {}_2I_4 Z_{22\,43} + {}_2I_1 Z_{22\,13} + {}_2I_2 Z_{22\,23} + {}_2I_3 Z_{22\,33} \,. $$

Reference to Fig. II-2 shows that many of these mutual impedances are the same: $Z_{11\,44} = Z_{11\,33} = Z_{11\,22} = Z_{11\,11} = Z_{22\,44}$

$= Z_{22\,33} = Z_{22\,22} = Z_{22\,11}$, $Z_{11\,41} = Z_{11\,12} = Z_{11\,23}$

$= Z_{11\,34}$, $Z_{11\,42} = Z_{11\,13}$, $Z_{22\,41} = Z_{22\,12} = Z_{22\,23}$

$= Z_{22\,34}$, $Z_{22\,42} = Z_{22\,13}$, $Z_{12\,44} = Z_{12\,11}$

$= Z_{12\,22} = Z_{12\,33}$, $Z_{12\,41} = Z_{12\,12}$

$= Z_{12\,23} = Z_{12\,34}$, and $Z_{12\,42} = Z_{12\,13}$.

Now, if taking the first four equations of (9), the set of voltages

$$ {}_1V_i = V^{(1)} \cos \left(\frac{\pi}{2} i - \phi_o\right) \qquad (10)$$

is applied to the first ring, and the second ring is made parasitic, (9) can be solved for the currents. After considerable manipulation the results are found to be

$$ {}_1I_i = \frac{V^{(1)} \cos\left(\frac{\pi}{2} i - \phi_o\right)}{{}_{11}Z^{(1)} - \frac{\left[{}_{12}Z^{(1)}\right]^2}{{}_{22}Z^{(1)}}} , \tag{11} $$

and

$$ {}_2I_i = - {}_1I_i \frac{{}_{12}Z^{(1)}}{{}_{22}Z^{(1)}} . \tag{12} $$

In (11) and (12) ${}_{11}Z^{(1)}$ and ${}_{22}Z^{(1)}$ are the one-sequence impedances of the first and second rings respectively, as given by (12). ${}_{12}Z^{(1)}$ is called the one-sequence mutual impedance between the rings, and has exactly the same form as (12), except that the distances are those between the first and second rings. It is seen that the induced currents have the same form as the currents in the driven ring, and consequently will radiate the same shape pattern.

If there is no offset between the rings, the pattern will be

$$ F^{(1)}(\theta,\phi) = j \frac{4V^{(1)}}{{}_{11}Z^{(1)} - \left[{}_{12}Z^{(1)}\right]^2 / {}_{22}Z^{(1)}} \left[J_1(\beta\rho_1 \sin\theta) - \frac{{}_{12}Z^{(1)}}{{}_{22}Z^{(1)}} J_1(\beta\rho_2 \sin\theta) \right] \cos(\phi - \phi_o) . \tag{13} $$

If there is an offset, the only result is displace the final pattern by an amount that depends on the offset angle α .

Finally, consider the case where the second ring contains eight elements. This can be resolved into three groups, each consisting of four elements, as shown in Fig. II-3, and analyzed as above. The result is that both a one-sequence and a three-sequence current is induced in the second ring; the one-sequence being the sum of the one-sequences of the four-element sub-groups, and the three sequence being the difference. However, if $\beta\rho_2 = 2$, $J_3(2)$ is small, and the three sequence is not radiated appreciably.

If the center element in the two-ring array of Fig. II-3 is driven, a zero-sequence is induced in each of the three four-element groups. It is then found that the zero-sequence component of the second ring is the sum of the zero-sequence components of the sub groups, and that a four-sequence component equal to their difference is also present. However, since $J_4(2)$ is small, it does not radiate.

Lastly, if the outer ring is driven in the two sequence, a set of two sequence currents is induced in the inner ring.

As a check on this theory of sequence coupling, the mutual impedance matrix of the array of Fig. II-3 was inverted using a digital computer, and all of the currents were found when the inner ring was driven so as to point the beam to 0^o, 22.5^o and 45^o. The exact patterns were then calculated, using the computer, and are shown in Fig. II-4. The only effect of the mutual coupling is to slightly change the size by about 1.5 db with angle of scan. Experimental verification is given in section IV.

C. Concentric Ring Scanning Antenna

The preceding sections contain all of the theory needed to design a concentric ring, scanning antenna. The array will contain K rings, numbered from k = 1 to k = K, each ring having 4k elements, and a circumference $\beta\rho = k$. Each ring is fed from two controlled amplifiers, the control voltages being $\cos k\phi_o$ and $\sin k\phi_o$, and the amplifier outputs $V^{(k)} \cos k\phi_o$ and $V^{(k)} \sin k\phi_o$. Appropriate transmission line networks then can be used to make the terminal voltages have the form

$$V_i^{(k)} = V^{(k)} \cos\left(\frac{\pi}{2} i - k\phi_o\right), \quad (1)$$

and the pattern, including the effect of currents induced in the other rings is

$$F^k(\phi) = A_k \cos k(\phi - \phi_o), \quad (2)$$

where $A_k = CV^{(k)}$, C being some constant involving a great number of parameters, including the mutual impedances, Bessel functions of the circumferences, and generator impedances. The final pattern is then of the form

$$F(\phi) = \sum_{k=0}^{K} A_k \cos k\phi. \tag{3}$$

The constant term is supplied by an element at the center.

For directional patterns with low side-lobe levels, the use of Tchebyscheff polynomials gives a good way to select appropriate values of A_k. The method for accomplishing this was given by DuHamel[4], and is also to be found outlined in considerable detail in Scientific Report Number 4 on this contract. The required numbers of rings, elements, and amplifiers to obtain various beamwidths are given in Table II-3.

Table II-3

Required numbers of rings, elements, and amplifiers for various half-power beamwidths and side-lobe levels.

Number of rings	Number of Elements	Number of Amplifiers	Beamwidth in Degrees	
			20 db side-lobe	30 db side-lobe
1	5	3	125	130
2	13	5	74	83
3	25	7	51	60
4	41	9	40	46
5	61	11	32	38
7	113	15	22	27
10	221	21	16	18
80	12961	161	2	2

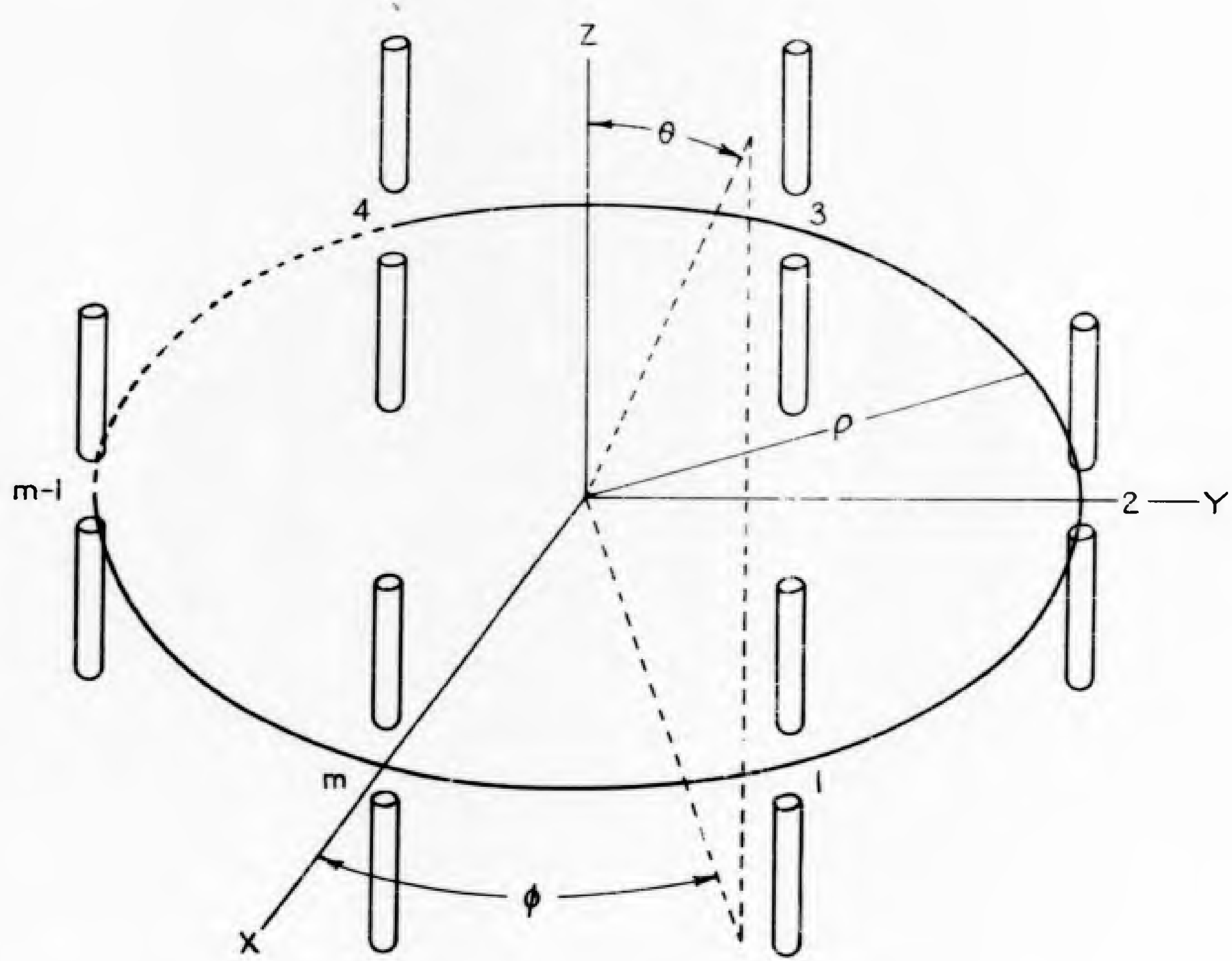

Fig. II-1. Coordinate system used in analysis of circular arrays.

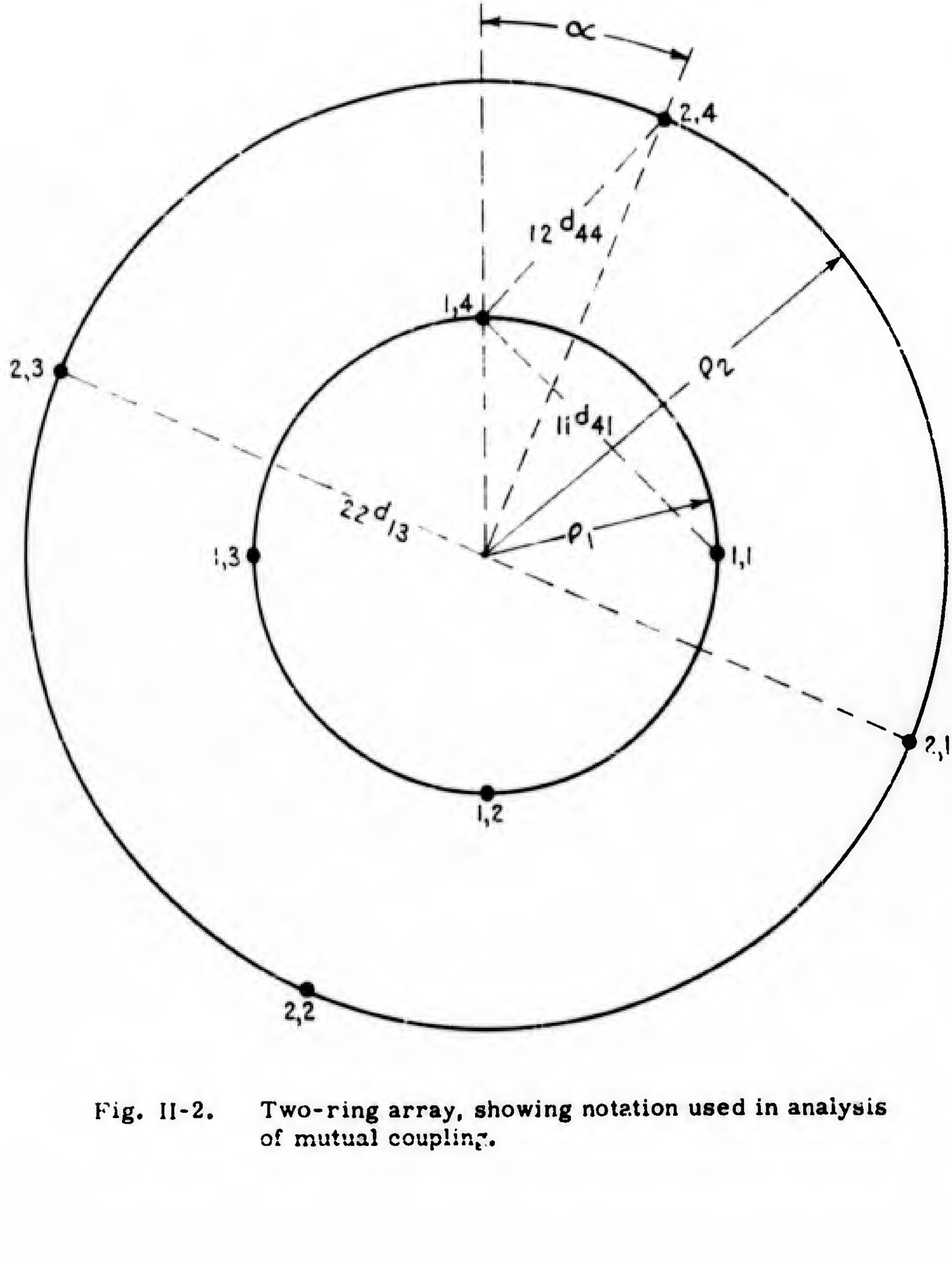

Fig. II-2. Two-ring array, showing notation used in analysis of mutual coupling.

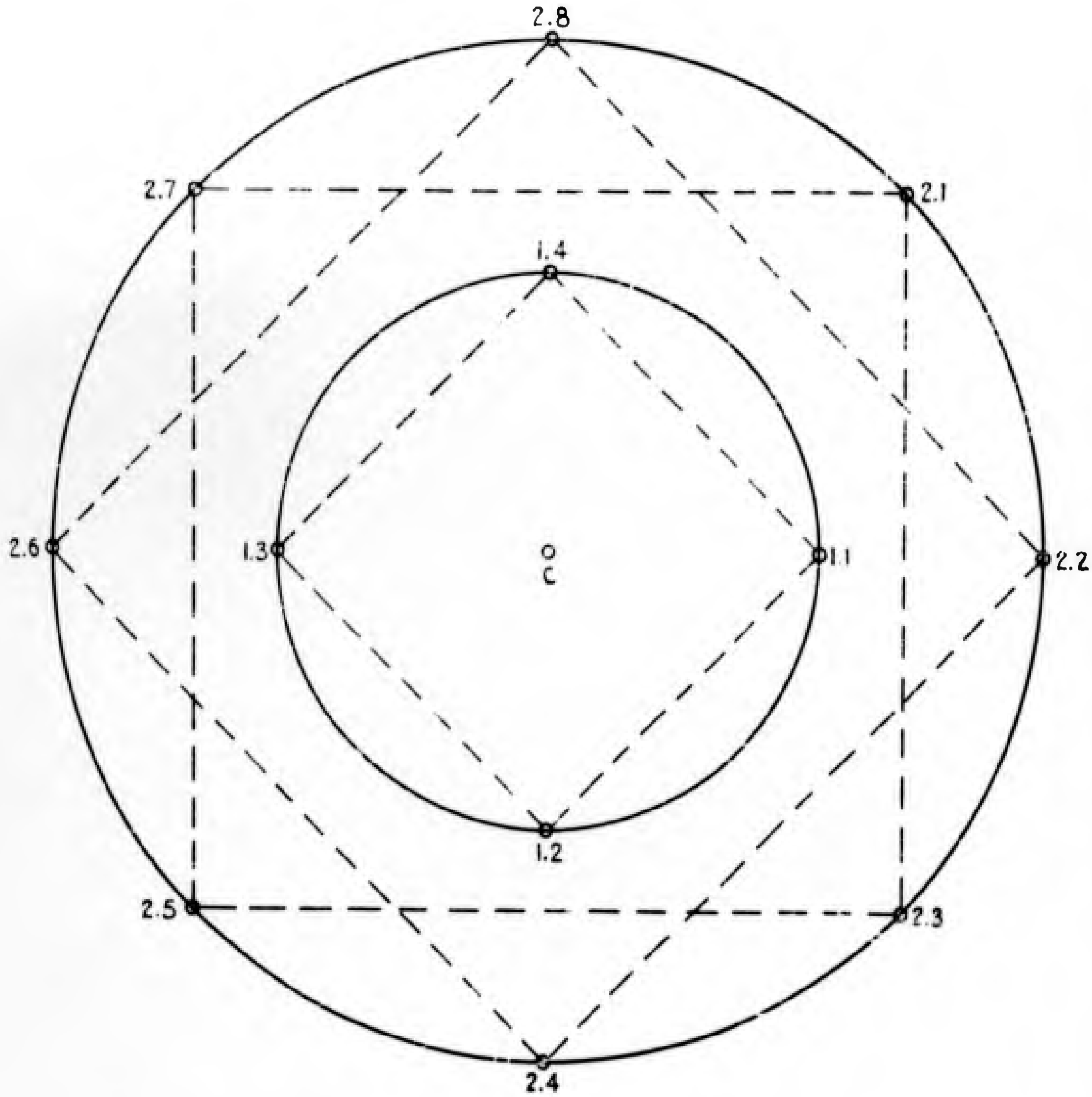

Fig. II-3. Plan view of two-ring array with center element, showing 4-element groups.

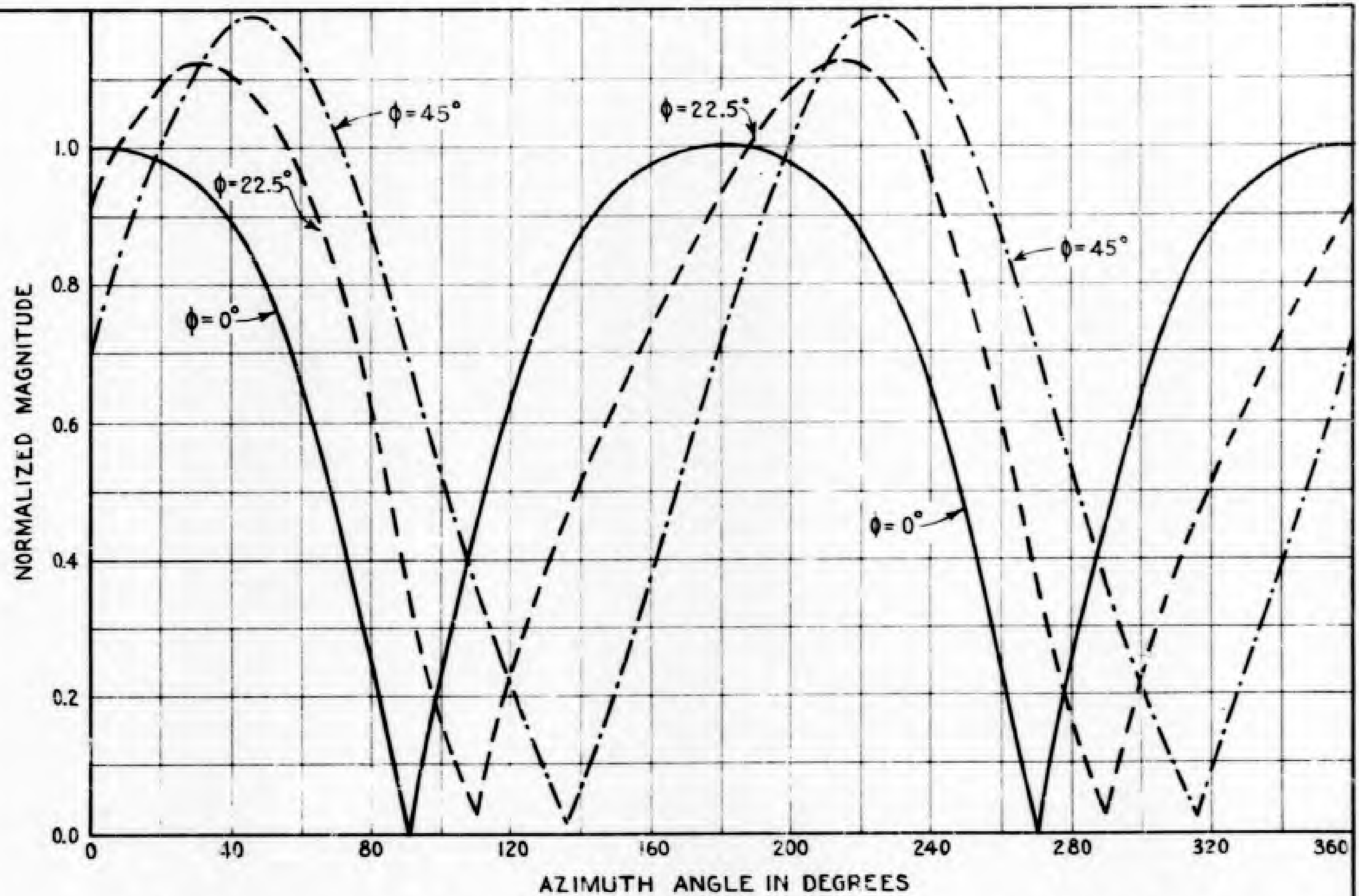

Fig. II-4. Computer solution for the pattern of Fig. II-3, when excited to give a pattern cos $(\phi-\phi_o)$.

III. EXCITATION SYSTEM FOR THE SCANNING ARRAY

The general theory of the electronic scanning circular array was set out in the preceding section. In order to obtain experimantal verification of this theory, and to investigate the associated electronic equipment, an antenna of this type was constructed and tested. This section describes the electronic portion of the system.

It was decided that an array having three or four rings would be large enough to prove the feasibility of the scanning method, so the electronics package was designed to provide the proper terminal voltages for a four ring system. A carrier frequency of 300 megacycles per second was chosen as being reasonable for the antenna test range on which patterns were to be measured. The antenna itself was constructed using quarter-wave monopoles, so the outputs of the electronic package and the power dividing and feeding system were all coaxial. The system was designed to be operated in two ways: fixed pointing, in which the shape of the pattern is determined by externally applied d.c. voltages; and scanned, in which a directional beam is rotated at a speed of 60 revolutions per second. In the scanning mode, the shape of the pattern is monitered on a oscilloscope, and controls are provided so that shape may be changed as desired.

A. General organization.

In Section II it was shown that a set of voltages

$$V_i^{(k)} = V^{(k)} \cos \left(\frac{2\pi}{m} ki - k\phi_o \right) \tag{1}$$

give rise to a pattern at $\theta = \pi/2$ given by

$$F^{(k)}(\phi) = j^k \frac{V^{(k)}}{Z^{(k)}} J_k(\beta\rho) \cos k(\phi - \phi_o) . \tag{2}$$

If m = 4k, (1) reduces to

$$V_i^{(k)} = V^{(k)} \cos \frac{\pi}{2} i \cos k\phi_o \quad , \qquad i \text{ even,}$$

$$= V^{(k)} \sin \frac{\pi}{2} i \sin k\phi_o \quad , \qquad i \text{ odd.} \tag{3}$$

To drive the elements of such a ring only two amplifiers are needed, with output voltages of $V^{(k)} \cos k\phi_o$, and $V^{(k)} \sin k\phi_o$. For a uniformly rotating beam, $\phi_o = \omega_s t$, where ω_s is the angular velocity with which the beam rotates. If the instantaneous value of the carrier is included, the required voltages are

$$V^{(k)} \cos k\omega_s t \cos \omega_c t$$

$$= \frac{V^{(k)}}{2} \left[\cos (\omega_c + k\omega_s t) + \cos (\omega_c - k\omega_s t) \right] , \tag{4}$$

and

$$V^{(k)} \sin k\omega_s t \cos \omega_c t$$

$$= \frac{V^{(k)}}{2} \left[\sin (\omega_c + k\omega_s t) - \sin (\omega_c - k\omega_s t) \right] . \tag{5}$$

Now (4) and (5) are readily recognized as the expressions for suppressed carrier amplitude modulated waves. The required voltages given by (3) can thus be generated by the use of balanced modulators.

There is a factor j^k in (2), so to make the contributions from each ring add in phase as explained in Section II, the currents in each ring must differ in phase by 90^o from the currents in the adjacent ring. Since both the balanced modulation and this phase shift are more easily obtained at low frequencies than at 300 mc, it was decided to carry out the control operations at 30 mc. Then the output of the modulated amplifier can be mixed with the output of a 270 mc source, and the sum frequency amplified in a 300 mc linear amplifier.

A block diagram of the resulting system is shown in Fig. III-1. A 7.5 mc crystal controlled source is doubled twice in frequency, to 30 mc, and this voltage is applied to all eight channels. A 30 mc buffer amplifier drives the balanced modulator, which is followed by another buffer. This is in turn followed by the mixer, and then by a 300 mc linear amplifier. The phase shifter is incorporated in the first buffer amplifier block. The modulating voltages for the eight channels are $\cos\phi_o$, $\sin\phi_o$, $\cos 2\phi_o$, $\sin 2\phi_o$, $\cos 3\phi_o$, $\sin 3\phi_o$, $\cos 4\phi_o$, and $\sin 4\phi_o$. Two channels then feed each ring. The first two channels feed the k = 1 ring, the output of each amplifier being split between two elements. In the k = 2 ring, each amplifier feeds four elements; for k = 3 each amplifier feeds 6 elements; and in general, each amplifier must feed 2k elements.

Since $\phi_o = \omega_s t$, a source is needed to supply voltages $\cos\omega_s t$, $\sin\omega_s t$, $\cos 2\omega_s t$, $\sin 2\omega_s t$,----- $\sin 4\omega_s t$ to the modulator. Gain controls incorporated at this point can be used to control the shape of the pattern.

B. Radio-Frequency Section.

A schematic diagram of the radio-frequency part of the system is shown in Fig. III-2. The 7.5 mc crystal oscillator and the frequency doublers, which are not included in Fig. III-2 are entirely conventional. The control of the phase is accomplished by the potentiometer in the plate circuit of the first 6AU6 tube. The impedance of this circuit is constant in magnitude, but varies in phase by almost 180^o as the potentiometer is varied from one extreme to the other. The second 6AU6 is a driver for the balanced modulator. A modulator using diodes was chosen because it offered the advantages of simplicity, high carrier suppresssions and the ability to accept d.c. modulating voltages, thus making it possible to stop the beam at a fixed angle of pointing. The 6AG7 serves as a class A buffer amplifier. The 6360 is the mixer. The signal from the 270-mc local oscillator, which is also crystal controlled is fed into the grid, and the suppressed carrier signal at 30 mc is coupled into the cathode. The plate circuit is then tuned to 300 mc, the sum frequency. The final power amplifier, a 6939, is normally operated class A, and delivers a power of about 2 watts. An amplitude control is incorporated in the screen circuit of this stage.

The r-f channels, besides the necessary tuned circuits, have three controls. These are:

1. Phase shift-accomplished in the first stage.
2. Carrier suppression-accomplished in the modulator.
3. Amplitude-accomplished in the final stage.

The three controls are virtually non-interacting. Almost a full 180° variation in phase can be obtained, and about 30 db of carrier suppression is readily achieved.

C. Sequence Generator.

A generator is required to produce the control voltages $\cos \omega_s t$, $\sin \omega_s t$, $\cos 2\omega_s t$, --- $\sin 4\omega_s t$. The requirements on this generator are: output voltages at 60 cps, 120 cps, 180 cps, and 240 cps; and at each frequency, two outputs 90° different in phase. The frequencies must be exact multiples of the fundamental. Controls must be provided to balance the two outputs at each frequency, to adjust the phase difference between these outputs to exactly 90°, to change the amplitude of both outputs together, and to change the phase of both outputs together.

The 60 cps line frequency is used to provide the one-sequence, to insure stability. The two-sequence is obtained from the one-sequence by full-wave rectification, followed by bandpass filtering at 120 cps. The second harmonic of this full-wave signal is at 240 cps, and is used to obtain the four-sequence by filters. A 60 cps square wave is obtained by clipping the one-sequence, and the third harmonic of this square wave is selected by a 180 cps filter. The harmonic content of the sequence voltages after filtering was measured, and found to be less than 5%. Two precautions were taken to prevent interactions between sequences. The filament circuits were operated from a d.c. supply, and the plate circuits were decoupled.

A phase shift control was next provided so that each sequence could be adjusted in phase with respect to the one-sequence. Each channel was next split into a two-phase system by a balanced R-C bridge to provide $\cos k\omega_s t$ and $\sin k\omega_s t$. The balance control is also incorporated at this point. The amplitude control is part of the last amplifier, which works in a step-down transformer to provide a low impedance output for cables to the balanced modulator.

The circuit diagram of this control generator is shown in Fig. III-3, and an oscillogram showing the output wave shapes is given in Fig. III-4.

D. Stability of the Excitation System.

An organized method is needed to adjust any device having as many independent controls as does the excitation system for the scanning array. The following procedure was used:

1. The controls of the sequence-control generator were adjusted so that the cosine and sine outputs of each channel were balanced.
2. Each channel of the sequence control generator, was brought in phase with the one-sequence output, and the amplitudes of all channel outputs were made equal.
3. The balanced modulators were adjusted to give maximum carrier suppression.
4. The sequence-control generator outputs were connected to the balanced modulators, and the r-f gain controls were adjusted to give equal r-f outputs from each channel.

The excitation system was now ready to test. After carrying out these steps, the r-f outputs are all proportional to the sequence-control voltages, and if these voltages are added by a summing amplifier, the resulting wave shape is the shape of the radiation pattern. For use with the antenna, the amplifiers are next connected to the transmission line network connecting to the antenna terminals.

A number of tests were made at this point, using dummy loads. The first set of tests involved only the 30-mc part of the system. The outputs of the last 30-mc buffers were connected to a five arm resistive power divider (Microlab DC-3), which was used as a summing device to simulate the antenna. The 30-mc output, its detected envelope, and the sum of the sequence-control voltages were all monitored simultaneously on a Tektronix dual-beam oscilloscope. This test set up is shown in Figs. III-5 and III-6. Actually, only three channels of the system were used; enough to obtain a $T_2(\phi)$ pattern. The amplitude and phase of these three terms, A_o, $A_1 \cos\phi$, and $A_2 \cos 2\phi$ were then adjusted using the amplitude control on the sequence generator, and the phase control ahead of the balanced modulator, until a pattern with 20-db side lobes was obtained. The system was allowed to warm up for one hour, then carefully readjusted. Fig. III-7 shows the wave shapes at 9:50 AM at the start, at 3:40 PM when the system was turned off, and at 5:05 PM. 45 minutes after it was turned back on, with no readjustments. The stability is seen to be quite good.

A second stability test was made which included the 300-mc part of the system. The set up was quite similar, the outputs of three 300-mc channels being summed in the resistive divider. Since the oscilloscope could not reproduce a 300-mc wave, the output from the divider was mixed with the output of the same 270-mc local oscillator used to mix up to 300 mc. The 30-mc difference frequency was then monitored on the oscilloscope. Fig. III-8 shows the wave forms at 10:00 AM, after an hour's warm up, and at 3:00 PM. Only the 30-mc signals are shown. The stability is again seen to be quite good.

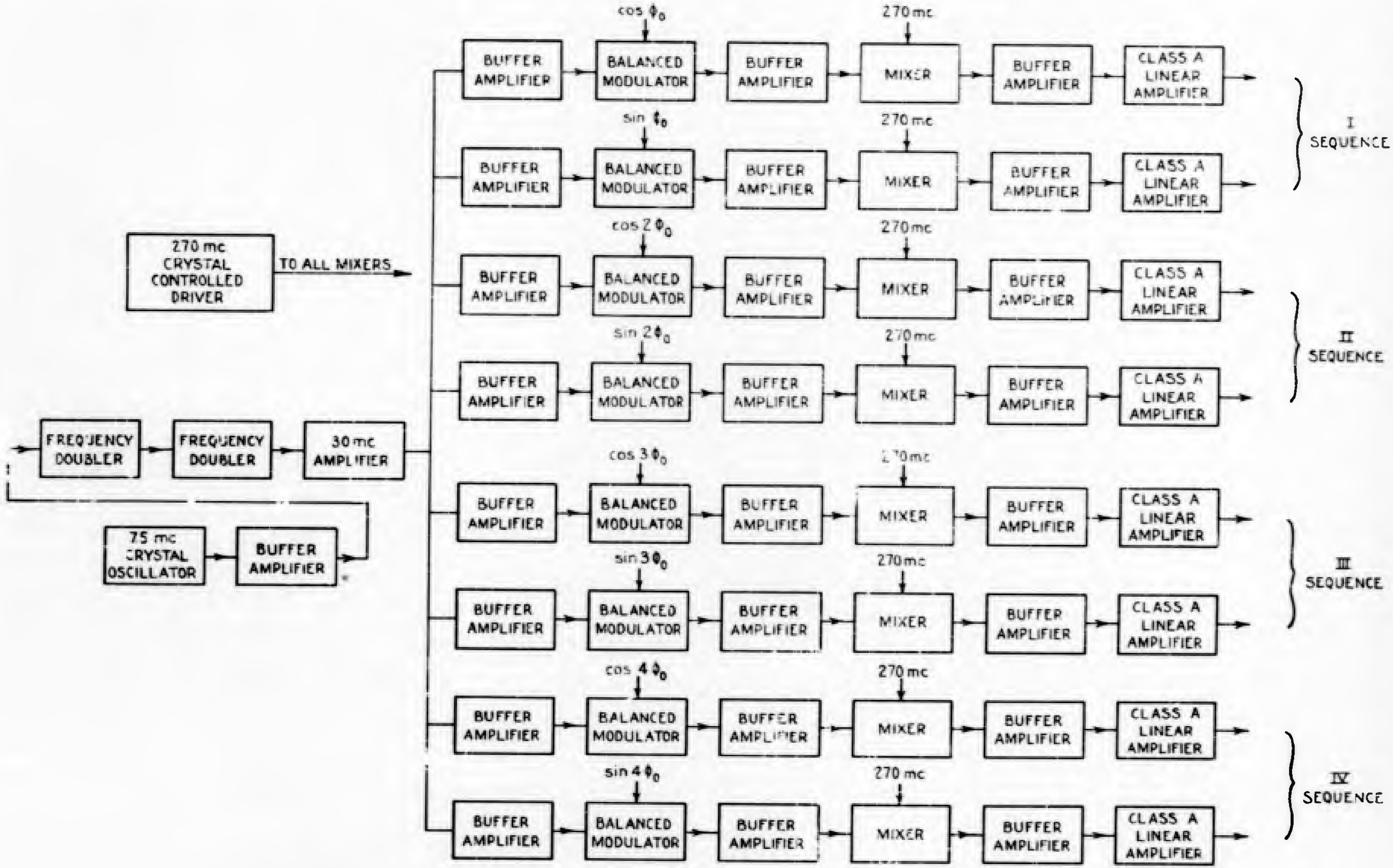

Fig. III-1. Block diagram of the electronic system for the scanning circular array.

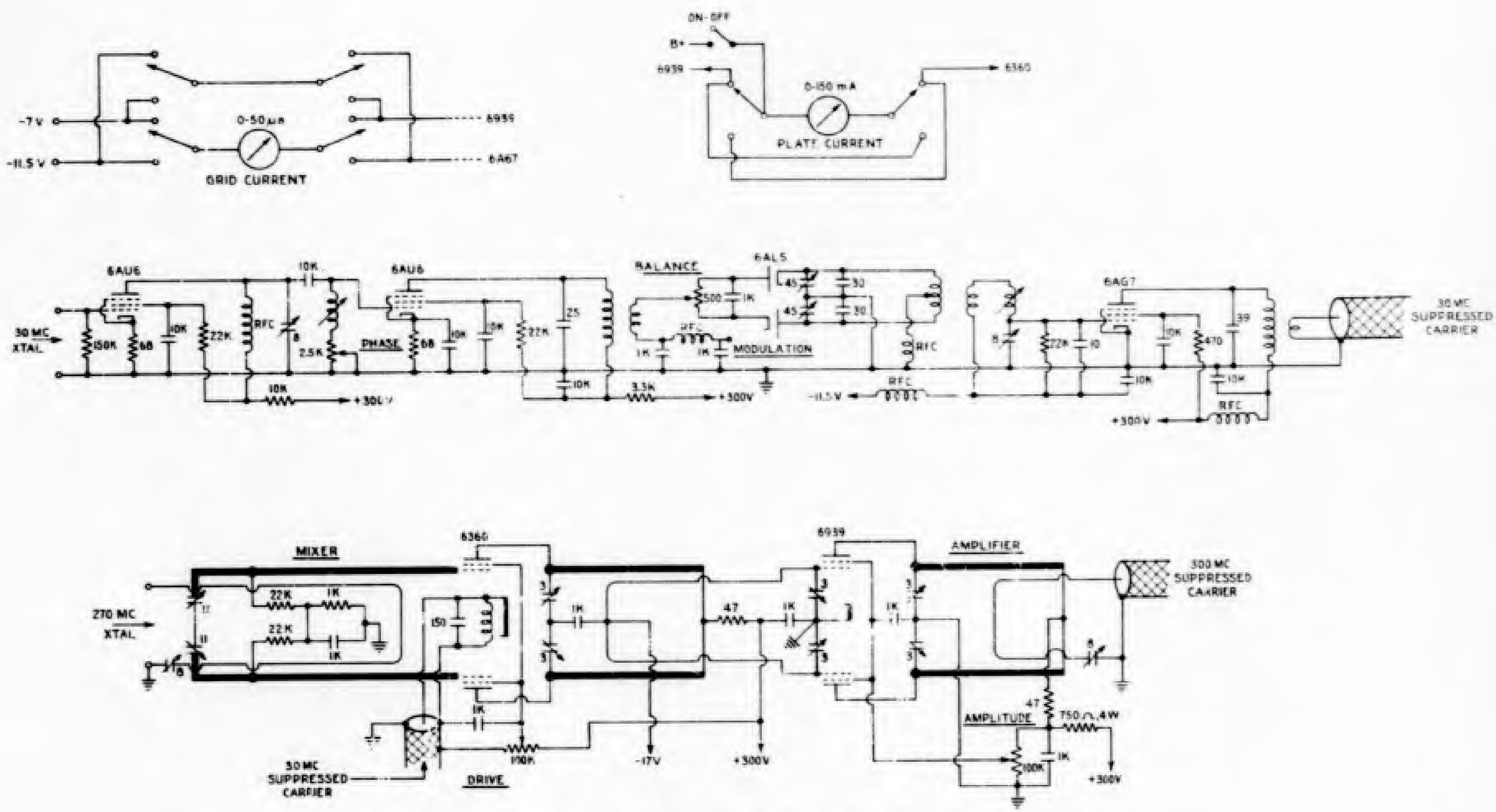

Fig. III-2. Schematic circuit of the radio-frequency section.

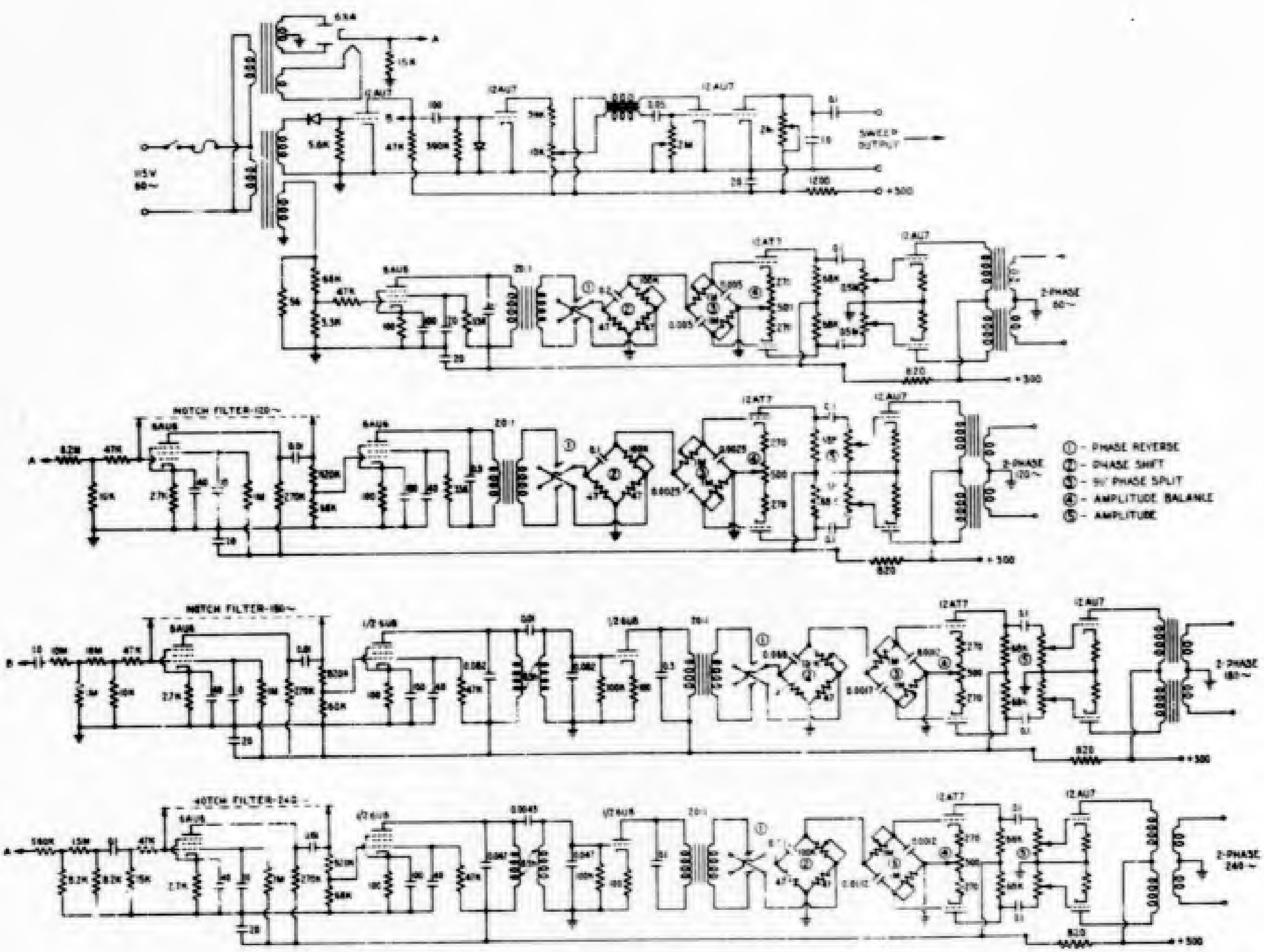

Fig. III-3. Schematic circuit of the sequence-control generator.

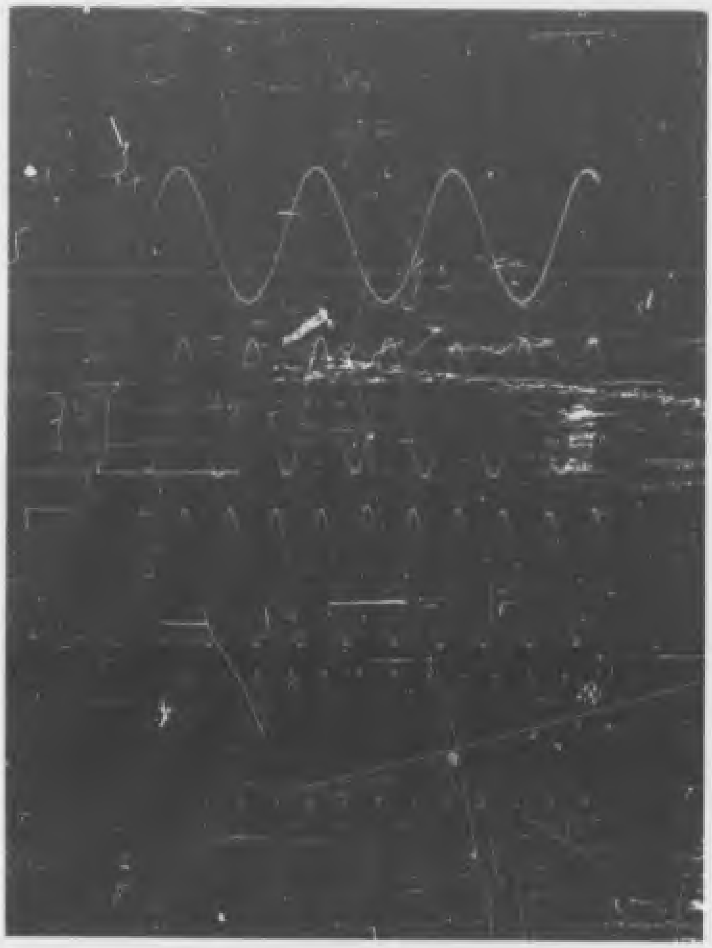

Fig. III-4. Output voltages of the sequence-control generator.

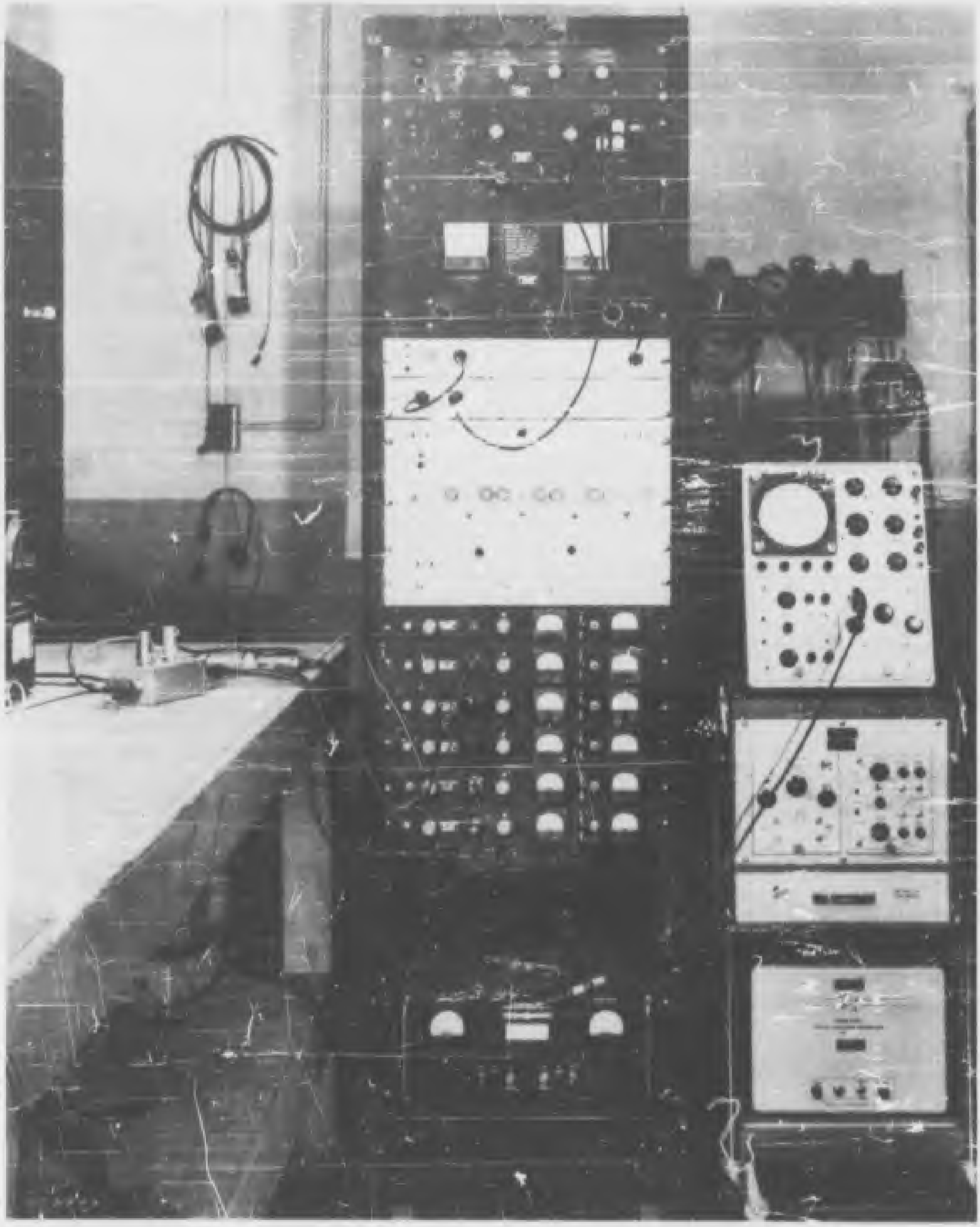

Fig. III-5. Front view of the electronic system as assembled for stability tests.

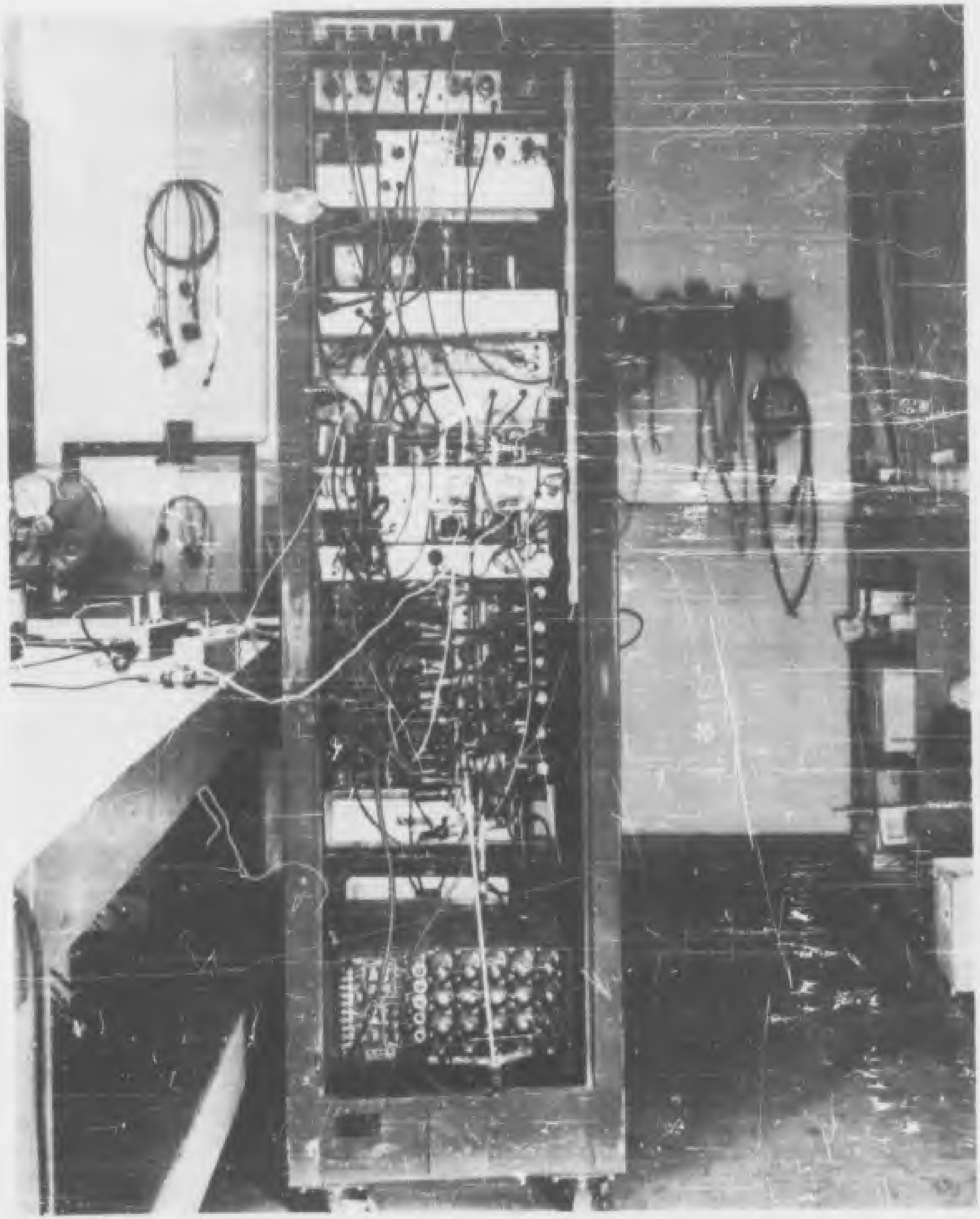

Fig. III-6. Rear view of the electronic system.

Fig III-7. Stability test of the 30-mc part of the electronic system, adjusted to give a $T_2(\phi)$ pattern. Top: 9:50 AM, middle: 3:40 PM, bottom: 5:05 PM.

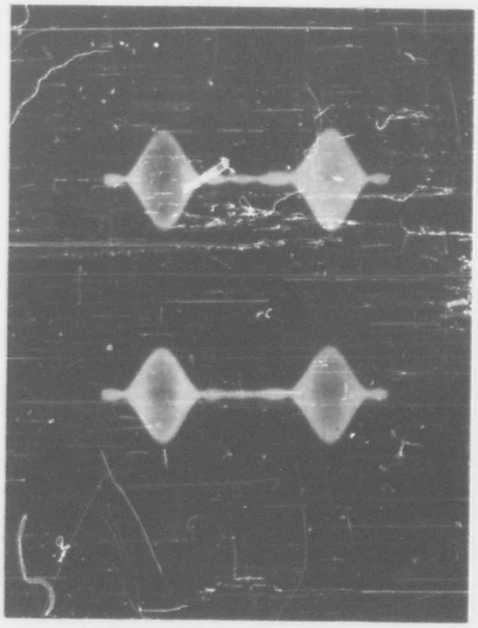

Fig. III-8. Stability test of the entire electronics system. Top. 10:00 AM, Bottom: 3:00 PM.

IV. PERFORMANCE OF THE SCANNED ARRAY

The electronics package described in section III can be used to drive circular scanning arrays having one, two, three, or four rings, and a central element. This section gives the results of rather extensive tests of a two-ring array, and also includes patterns for a three-ring array. In addition to pattern measurements, the two-ring array was used to study experimentally the effects of mutual coupling between rings.

A. Method of Excitation.

A photograph of the antenna is shown in Fig. IV-1. The array consists of quarter-wave monopoles, each of which is an extension of the center conductor of a transmission line through the ground plane, via a connector. There is an element at the center of the array, and the concentric rings consist of four, eight, and twelve elements, the rings having circumferences of one, two, and three wavelengths, respectively. The lower end of the elements is threaded, so that they may be unscrewed from the coaxial fittings set in the ground plane.

Fig. IV-2 is a photograph showing the transmission line network which feeds the array. The 1-sequence ring contains four elements, for which the terminal voltages should be

$$\begin{aligned} V_4 &= V^{(1)} \cos\phi_o \\ V_2 &= -V^{(1)} \cos\phi_o \\ V_1 &= V^{(1)} \sin\phi_o \\ V_3 &= -V^{(1)} \sin\phi_o \end{aligned} \qquad (1)$$

The output of channel No. 1, Fig. III-1, is $V^{(1)} \cos\phi_o$. This is connected to a two-way reactive power divider by a transmission line, and the outputs of the power divider are connected to elements 4 and 2 by transmission lines of length $\lambda/4$ and $3\lambda/4$ respectively. Elements 1 and 3 are fed from channel No. 2, Fig. III-1 by an identical arrangement. Consideration of this scheme shows that this insures the correct currents in this ring. Table IV-1 shows the connection scheme for all three rings. It is evident that four-way power dividers are needed in the two ring, and six-way dividers in the three ring.

Table IV-1. Feed connections for three-ring array.

Ring Number	Channel Number	Control Voltage	Element Number	Line Length
1	1	cos ϕ_o	4	$\lambda/4$
			2	$3\lambda/4$
	2	sin ϕ_o	1	$\lambda/4$
			3	$3\lambda/4$
2	3	cos 2 ϕ_o	2,6	$3\lambda/4$
			4,8	$5\lambda/4$
	4	sin 2 ϕ_o	3,7	$3\lambda/4$
			1,5	$5\lambda/4$
3	5	cos 3 ϕ_o	2,6,10	$3\lambda/4$
			12,4,8	$5\lambda/4$
	6	sin 3 ϕ_o	1,7,11	$3\lambda/4$
			1,5,9	$5\lambda/4$

Fig. IV-3 is another photograph of the feed system, from a large enough distance to include the electronics package. The power dividers are all mounted in the box directly under the antenna, and coaxial connectors on the side of the box connect to lines to the electronics package. The length of these lines is not critical, since there are phase and amplitude adjustments in each channel of the electronics section.

The procedure used to adjust all of the controls properly is very similar to that outlined in section III, the difference being in step 4. To adjust the one-sequence ring, two pickup antenna are needed, one lying on a radial through element No. 4, and one in line with element no. 2. Step 4 now becomes:

4. The sequence-control generator outputs were connected to the balanced modulators, and the r-f gain controls in channels 1 and 2 were adjusted to give equal outputs from each pickup antenna.

5. Each ring is now brought into balance in this same way, using two pickup antennas, one in line with an element in the odd channel group of elements, the other in line with one of the remaining antenna elements. The signal at the pickup antennas must be the same as each ring is excited alone.

This procedure makes the radiated pattern, including the Bessel function factor, and any induced currents, vary directly with the voltage from the sequence-control generator. Thus the pattern formed by summing these voltages is the same as the radiated scanning pattern.

B. Coupling Between Rings.

In section II, a theoretical account of the coupling between rings was presented. A summary of the results follows:

1. There is no coupling between a ring and the center element when the ring is excited so as to give a pattern of the form $\cos k(\phi-\phi_o)$.

2. When a ring is driven so as to give a pattern of the form $\cos k(\phi-\phi_o)$, the currents induced in the other ring are predominantly such as to also give patterns of the form $\cos k(\phi-\phi_o)$.

Since the entire design of the scanned array is based on these theoretical conclusions, experimental confirmation of these properties of concentric ring systems was thought to be necessary, and a number of tests were made. A two-ring array was used for these tests. The inner ring was excited as described in IV-A, and the effect of induced currents was studied.

The first test involved the coupling to the center element. The outer ring was open circuited, so that no currents would be induced, and the inner ring driven to give a pattern of the form $\cos(\phi - \omega_s t)$. Pickup antennas were located on the $\phi=0$ and $\phi=135^o$ radials, the 300-mc recieved signals were mixed with a 270-mc local oscillator, and the resulting 30-mc difference frequency was examined using a dual beam oscilloscope. Figure IV-4 shows the resulting patterns. The center element was terminated in a variable-length 50-ohm air line, which was in turn terminated with a 200 ohm resistor. The three pairs of traces shown in Fig. IV-4 are for lengths of the air line of 30 cm, 45 cm, and 60 cm., respectively. Since the patterns are unchanged despite the changing termination on the center element, it follows that the center element carried zero current which was expected from the theory. A number of other tests with different terminations of the center element, including one in which the termination was continuously varried gave the same result. It is evident that properly driving the one-sequence ring does not induce a current in the center element.

In the second set of tests, the effect of the currents induced in the outer ring when the one-sequence ring was driven was studied. There are two effects which might occur: first, since there will be a small three-sequence current induced, a cos 3ϕ term in the pattern could be radiated, even though a ring with a circumference $\beta\rho = 2$ is an inefficient radiator of such a term; second, the one-sequence currents induced in the outer ring could be nearly out of phase with the driven currents in the one-ring, resulting in a small radiated field per unit current. The first effect should be very small; the second should indeed occur if the elements in the outer ring are shorted, but not if they are terminated in 50 ohms, as they are in actual operation.

Fig. IV-5 shows the patterns which resulted when the outer ring was terminated in a short circuit. The top pair of traces are for pick-up antennas at 0° and 45°, the middle pair for pick-up antennas at 0° and 22.5°, and the bottom pair are with the outer ring open, included for a reference. The center element was terminated in a short circuit. It is difficult to scale the results accurately from these photographs, but the effect of the presence of the shorted two ring is to reduce the size of the cos $(\phi-\phi_0)$ term by about 14 db. Fig. IV-6 is for the same situation, except that the elements in the two-ring are now terminated in 50 ohms. Inspection shows that the presence of the two-ring, terminated in 50 ohms, has almost no effect on the cos $(\phi-\phi_0)$ term. Fig. IV-6 should be compared with Fig. II-4, which gave the pattern calculated by the digital computer for this case, using the approximate zeroth-order impedances.

These tests indicate that the theoretical conclusions concerning coupling between rings are essentially correct, and that this coupling should not cause any difficulty.

C. Patterns of the Scanned Array.

Two-ring and three-ring versions of the scanning array were tested in actual operation. The adjustment of each ring was carried out in the manner described in section IV-A. The remaining adjustments concerned the amplitude of the contribution from each ring, and the phase of that contribution. These adjustments were made by observing the detected radiation pattern on the oscilloscope, and varying the phase and amplitude of the currents in each ring until the desired pattern was obtained.

A word of caution concerning the patterns of a 360° scanning array is is needed at this point. If only a pick-up antenna lying on the 0° radial is used, the field in this direction is due to the outputs of only channels 1, 3, and 5 of Fig. III-1. In the direction $\phi=90^{\circ}$, only channels 2,4, and 6 are involved. If two pick-ups are used, one at $\phi=0$, and one at $\phi=90^{\circ}$, the two sets of amplifiers can be adjusted correctly in amplitude, but may still not be phased correctly. Pick-ups at 0° and 45°, or at 0° and 135° are sufficient to insure a correctly scanning pattern. At this point, a practical difficulty was encountered due to the fact that the ground plane used for the measurements was of limited size. The pick-up antennas were located on the circumference of a circle about 7.5λ in radius. (The criterion of $2d^2/\lambda = 2\,(3\lambda/\pi)^2\,/\lambda = 1.8\lambda$ is thus more than met). But pick-up antennas at $\phi=0^{\circ}$ and $\phi=45^{\circ}$ are only spaced about 5λ from each other, and are mutually coupled to a slight degree. Patterns taken using this pair of pick-ups show a slight distortion not present in other patterns.

The two ring array was tested first. Figs. IV-7, IV-8, and IV-9 show the resulting patterns. They are, respectively, the patterns obtained with the pick-ups at 0° and 45°, 0° and 135°, and 0° and 180°. The side-lobe level is, in each case at least 20 db, and the beamwidth about 75°, which agrees very well with the calculated values.

Figs. IV-10, IV-11. and IV-12 show the results for the three ring system. They are the scanning patterns for pick-up antennas at 45°, 90°, and 135°. Each figure shows the way in which the pattern is built up. The top trace shows the contribution from only the center element, and the one-sequence ring; the middle trace shows the pattern when the contribution of the second ring is added, and the bottom trace shows the pattern of the entire array. Again the side-lobe level is about 20 db, and the beamwidth is about 50°, also in very good agreement with theory.

A very clear illustration of the properties of the scanned pattern was obtained by rotating the array using the turntable available for conventional pattern recording. Since the synchronization of the sweep for the oscilloscope was obtained from the sequence control generator, the scanned pattern moved across the face of the oscilloscope as the array rotated. The pattern did not change shape noticeably, showing that the shape of the scanned pattern does not change as the angle of pointing varies. Motion pictures of this were made, but, of course cannot be included with this report.

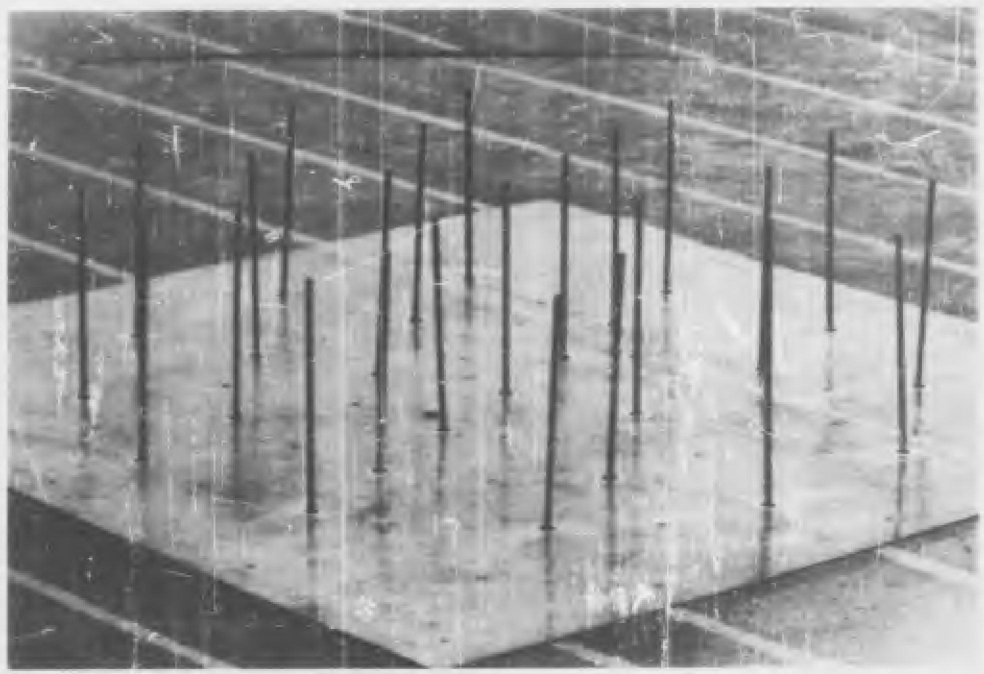

Fig. IV-1. Photograph of the an'enna array.

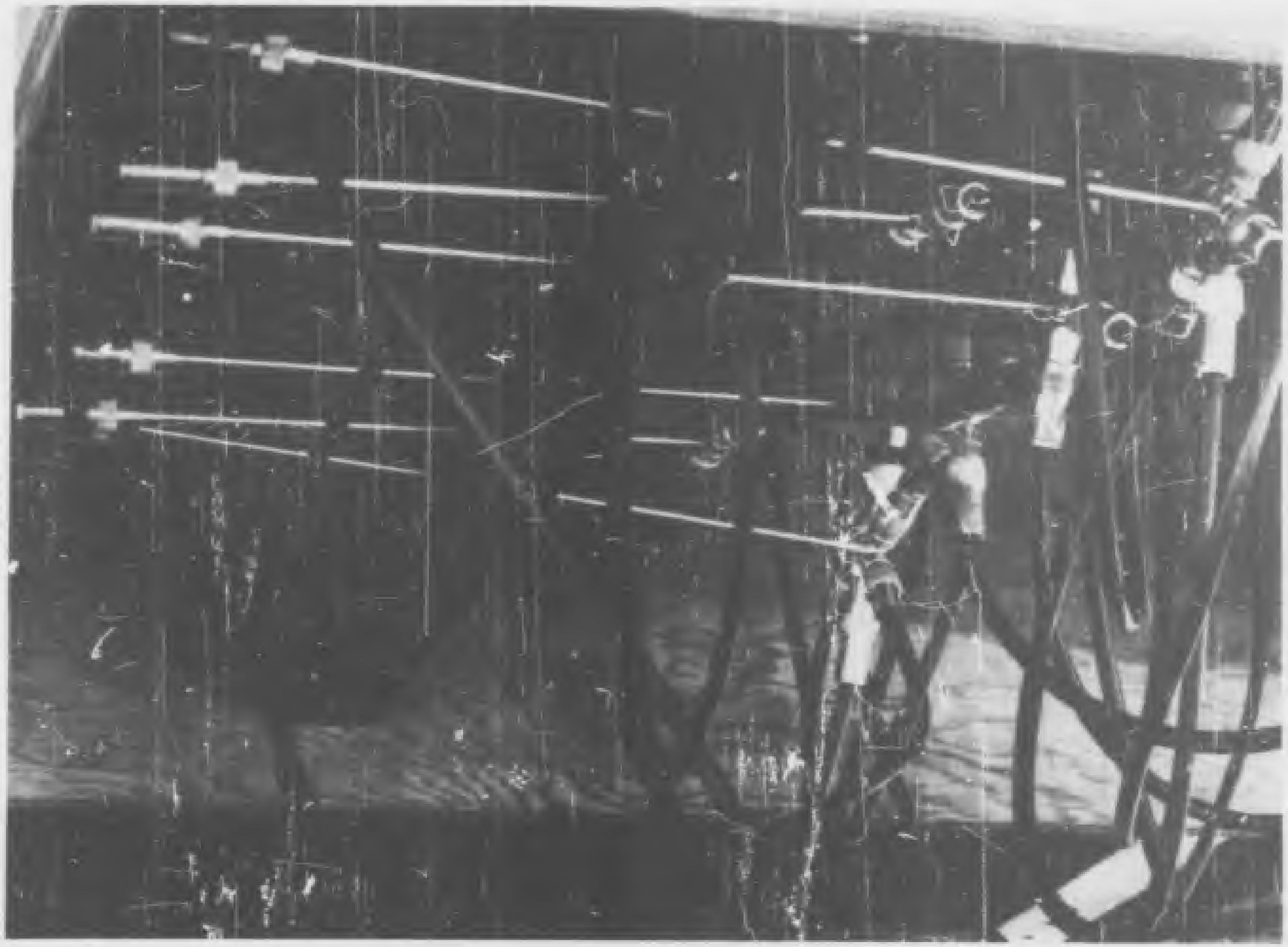

Fig. IV-2. Feed system of the scanning array.

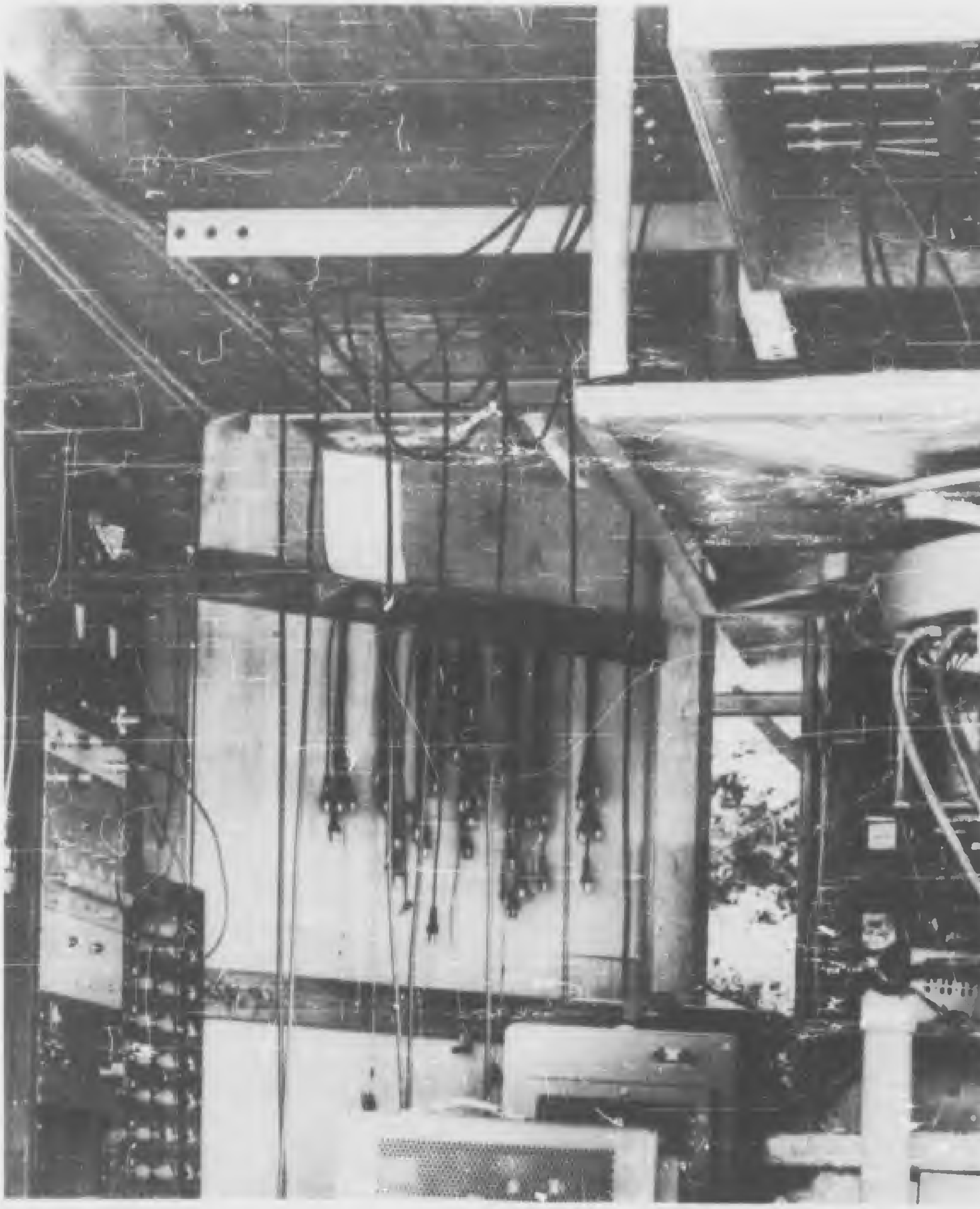

Fig. IV-3. Feed system, showing the electronic equipment.

Fig. IV-4. Patterns showing effect of mutual coupling to the center element.

Fig. IV-5. Patterns with one-sequence ring driven, center element and outer ring short circuited. Patterns at bottom are for one-sequence ring isolated.

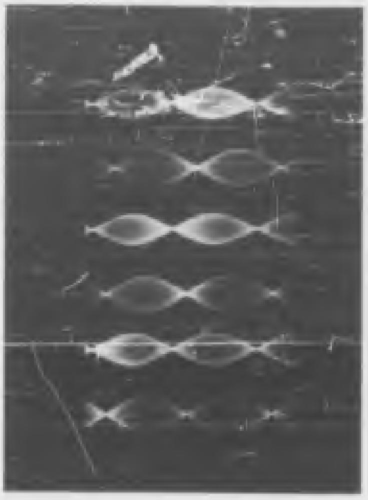

Fig. IV-6. Patterns with one-sequence ring driven, outer ring terminated in 50 ohms. Patterns at bottom are for one-sequence ring isolated.

Fig. IV-7. Scanning pattern of the two-ring array, pick-up antennas at 0° and 45°.

Fig. IV-8. Scanning pattern of the two-ring array, pick-up antennas at 0° and 135°.

Fig. IV-9. Scanning pattern of the two-ring array, pick-up antennas at 0^{o} and 180^{o}.

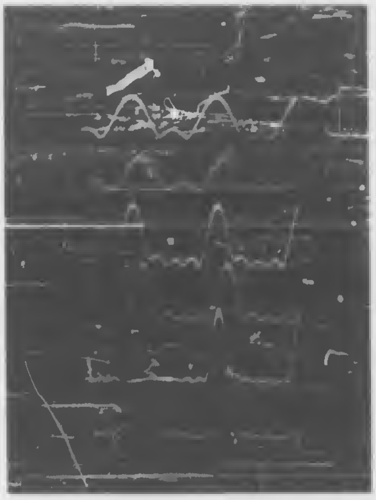

Fig. IV-10. Scanning pattern of the three-ring array with pick-up antenna at 45°.

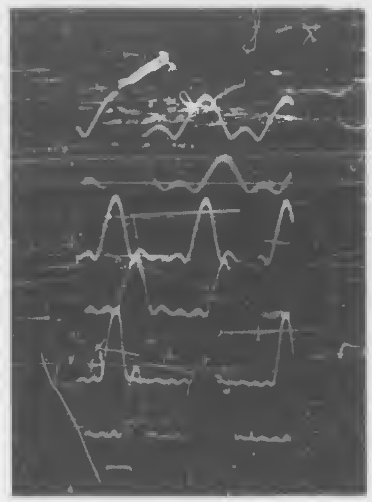

Fig. IV-11. Scanning pattern of the three-ring array with pick-up antenna at 90°.

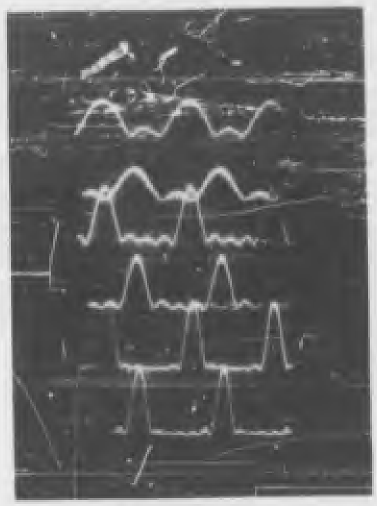

Fig. IV-12. Scanning pattern of the three-ring array with pick-up antenna at 135°.

V. CONCLUSIONS

This report has described an electronic scanning circular array, for which the beam can be pointed to any azimuth angle. The array, including the entire electronics package was built and tested, the performance agreeing very well with calculations.

The antenna has a number of properties which make it desirable for electronic scanning applications. Some of these are:

1. The beam can be scanned through a full 360° in azimuth without significant change in the shape of the pattern.
2. The voltages needed to control the direction of pointing are simple in nature. They can be obtained from an electronic system giving four-phase voltages at harmonics of the scan frequency, as described in this report, or from suitably coupled sine-cosine potentiometers if electro-mechanical control is desired.
3. The shape of the pattern can be adjusted very easily, and this shape can be monitored from the voltages controlling the direction of pointing.
4. The electronics system does not need any exotic circuitry, but instead is made up of an assembly of well-tested amplifiers, modulators, and mixers.
5. The same control system can be used for circular arrays designed for other frequencies. The only parts needing to be changed are the local oscillator, and the final linear radio-frequency amplifiers.
6. The sytem is moderately broadband. The array itself and the transmission line feed system could accomodate at least a 10% bandwidth, and the limiting factors are the bandwidths of the elements, and of the tuned circuits in the final amplifiers.
7. The problems caused by mutual coupling in many scanning arrays are not present. Mutual couplings are taken into account in the basic design.

These properties make this antenna system worthy of consideration for many electronic scanning applications.

REFERENCES

1. Stenzel, H., Uber die Richtcharakteristic von in einer Ebene Angeordneten Strahlern, Electrishe Nachrichten-Technik, Vol. 6, p 165, May 1929.

2. Knudsen, H. L., Bidrag Til Teorien for Antennesystemer med Hel Eller Delvis Rotationssymetri, I Kommission Hos Teknisk Forlag, Copenhagen, 1953.

3. DuHamel, R. H., Pattern Synthesis for Antenna Arrays on Circular, Eliptical and Spherical Surfaces, Technical Report No. 16, Electrical Engineering Research Laboratory, University of Illinois, Urbana, Ill., May 1952.

4. King, R. W. P., Theory of Linear Antennas, Harvard University Press, Cambridge, Mass., 1956, Chapter 3.

5. Hickman, C. E., Neff, H. P., and Tillman, J. D. , The Theory of a Single-Ring Circular Antenna Array, Transaction of AIEE, Vol. 80, Pt. 1, p. 110, May 1961.

6. Neff, H. P., Patton, W. T., Pierce, J. F., and Tillman, J. D., An Amplitude Scanned Circular Array, Final Report, Contract AF 19(604)-1557, Engineering Experiment Station, The University of Tennessee, Knoxville, Tenn., October 1958.

7. Neff, H. P., Patton, W. T., Pierce, J. F., and Tillman, J. D., "A Circular Array Suitable for Amplitude Scanning" International Scientific Radio Union, Spring Meeting, 1959.

8. Neff, H. P., and Tillman, J. D., An Electronically Scanned Circular Array, IRE Convention Record, Vol. 8, pt. 1, p. 41, 1960.

9. Hoffman, G. W. and Tillman, J. D. , Concentric Ring Antenna Arrays, AIEE Fall General Meeting 1961, paper CP 61-1179.

10. Mack, R. B., and Mack, E. W., Tables of E(h,z), C(h,z), and S(h,z), Cruft Laboratory Repprt No. 131, Harvard University, Cambridge, Mass., November 1960.

DISTRIBUTION LIST

Code	Organization	No. of Copies
AF 5	Commander Air Force Missile Test Center Patrick Air Force Base, Florida ATTN: Technical Library, MU-411	1
AF 13	Commander Air Research and Development Command Andrews Air Force Base Washington 25, D. C. ATTN: RDDL	1
AF 15	Commander Air Research and Development Command Andrews Air Force Base Washington 25, D. C. ATTN: Major E. Wright, RDTCC	1
AF 18	Director Air University Library Maxwell Air Force Base, Alabama	1
AF 28	Tactical Air Group Directorate of Research and Development, DCS/D Headquarters, USAF Washington 25, D. C. ATTN: Major R. L. Stell	1
AF 29	Commander Eglin Air Force Base Valpariso, Florida	1
AF 86	Commander-in-Chief Strategic Air Command Offutt Air Force Base Omaha, Nebraska ATTN: Operations Analysis Office	1
AF 63	Commander Wright Air Development Center Wright-Patterson Air Force Base, Ohio ATTN: Mr. Walter J. Portune, WCLRS-6	1
AF 43	Commander Wright Air Development Center Wright-Patterson Air Force Base, Ohio ATTN: WCRRA	1
AF 65	Commander Wright Air Development Center Wright-Patterson Air Force Base, Ohio ATTN: WCLNQ-4, N. Draganjac	1
AF 140	Commander Air Technical Intelligence Center Wright-Patterson Air Force Base, Ohio ATTN: AFCIN-4Bia	1
AF 142	Commander Wright Air Development Center Wright-Patterson Air Force Base, Ohio ATTN: D. H. Cartellano (WCRTR-4)	1
AF 124	Commander Rome Air Development Center Griffiss Air Force Base, New York ATTN: RCSSTL-1	1
AF 120	Commander Rome Air Development Center Griffiss Air Force Base, New York ATTN: Mr. Donald Dakan, RCUE	1
AF 143	Commander Rome Air Development Center (ARDC) Griffiss Air Force Base, New York ATTN: Dr. John S. Burgess, RCE	1
AF 139	Commander Air Force Missile Development Center Holloman Air Force Base, New Mexico ATTN: HDOIL, Technical Library	1
Ar 5	Director Evans Signal Laboratory Belmar, New Jersey ATTN: Technical Document Center	2
Ar 3	Director Evans Signal Laboratory Belmar, New Jersey ATTN: Mr. O. C. Woodyard	1
Ar 40	Director Evans Signal Laboratory Belmar, New Jersey Attn: S. Krevsky, Chief Microwave DF and Antenna Section	1
Ar 10	Massachusetts Institute of Technology Signal Corps Liaison Officer Cambridge 39, Massachusetts ATTN: A. D. Bedrosian, Room 26-131	1
Ar 49	Commanding General U. S. Army Signal Engineering Laboratories Fort Monmouth, New Jersey ATTN: SIGFM/EL-AT	1
Ar 39	Commanding General U. S. Army Signal Engineering Laboratories Fort Monmouth, New Jersey ATTN: Mr. F. J. Triola	1
Ar 9	Department of the Army Office of the Chief Signal Officer Washington 25, D. C. ATTN: SIGGD	1
Ar 41	Department of the Army Office of Chief Signal Officer Engineering and Technical Division Washington 25, D. C. ATTN: SIGNET-4	1
Ar 42	Director U. S. Army Ordnance Ballistic Research Laboratories Aberdeen Proving Ground, Maryland ATTN: Ballistic Measurements Laboratory	1
Ar 47	Ballistic Research Laboratories Aberdeen Proving Ground, Maryland ATTN: Technical Information Branch	1
Ar 48	Diamond Ordnance Fuze Laboratories Guided Missile Fuze Library Washington 25, D. C. ATTN: R. D. Hatcher, Chief, Microwave Development Section	1
G 2	Armed Services Tech. Information Agency Arlington Hall Station Arlington 12, Virginia	5
M 5	Hq Air Force Cambridge Research Center Air Research and Development Command Laurence G. Hanscom Field Bedford, Massachusetts ATTN: CROTLR-2, P. Condon	2
M 6	Hq Air Force Cambridge Research Center Air Research and Development Command Laurence G. Hanscom Field Bedford, Massachusetts ATTN: CROTLS, J. Armstrong	2
M 17	Hq Air Force Cambridge Research Center Air Research and Development Command Laurence G. Hanscom Field Bedford, Massachusetts ATTN: CRRD	5
N 1	Director, Avionics Division (AV) Bureau of Aeronautics Department of the Navy Washington 25, D. C.	1
N 3	Chief, Bureau of Ships Department of the Navy Washington 25, D. C. ATTN: Mr. E. Johnston, Code 833E	1
N 16	Commander U. S. Naval Air Missile Test Center Point Mugu, California ATTN: Code 366	1

DISTRIBUTION LIST

Code	Organization	No. of Copies
G 13	National Bureau of Standards Department of Commerce Washington 25, D. C. ATTN: Dr. A. G. McNish	1
G 27	National Bureau of Standards Department of Commerce Washington 25, D. C. ATTN: Gustave Shapiro, Chief, Engineering Electronics Section, Electricity and Electronics Division	1
G 6	Office of Technical Services Department of Commerce Washington 25, D. C. ATTN: Technical Reports Section	1
I 1	Airborne Instruments Laboratory, Inc. 160 Old Country Road Mineola, New York ATTN: Dr. E. G. Fubini, Director Research and Engineering Division	1
I 247	Bendix Radio, Division of Bendix Aviation Corporation East Joppa Road Towson 4, Maryland ATTN: Dr. D. M. Allison, Jr., Director Engineering	1
I 255	Dalmo Victor Company A Division of Textron, Inc. 1515 Industrial Way Belmont, California ATTN: Mary Ellen Addems, Technical Librarian	1
I 311	Hycon Eastern, Inc. 75 Cambridge Parkway Cambridge, Mass. ATTN: Mrs. Lois Seulowitz, Technical Librarian	1
I 8	Bell Aircraft Corporation Post Office Box 1 Buffalo 5, New York ATTN: Mrs. J. Mulcahey, Technical Librarian	1
I 48	Goodyear Aircraft Corporation 1210 Massillon Road Akron 15, Ohio ATTN: Russel V. Heath, Technical Service Dept. 463	1
I 50	Grumman Aircraft Engineering Corporation Bethpage, Long Island, New York ATTN: Chief Engineer	1
I 71	McDonnell Aircraft Corporation P. O. Box 516 Lambert St. Louis Municipal Airport St. Louis 3, Missouri ATTN: B. G. Bromberg, Missile Chief Engineer	1
I 82	Northrop Aircraft, Inc. Hawthorne, California ATTN: Northrop Library, Dept. 3145	1
I 157	Bendix Aviation Corporation Pacific Division 11600 Sherman Way North Hollywood, California ATTN: Mr. Stewart Leitch, Chief Engineer	1
I 158	Bjorksten Research Laboratories, Inc. Post Office Box 265 Madison, Wisconsin ATTN: H. R. Worthington, Jr.	1
I 161	Cornell Aeronautical Lab., Inc. Post Office Box 235 Buffalo, New York ATTN: Bureau of Aeronautics Representative	1
I 162	Corning Glass Works Corning, New York ATTN: M. R. Shaw, Applications Engineer Electronic Component Dept.	1
I 166	The Emerson Electric Manufacturing Co. 8100 Florissant Avenue St. Louis 21, Missouri ATTN: Sta. 270, Mr. C. G. Gulledge	1
I 177	Radio Corporation of America Camden 2, New Jersey ATTN: Clarence A. Gunther, Chief Defense Engineer, DEP Bldg. 15, Floor 7	1
I 185	Douglas Aircraft Company, Inc. El Segundo Division 827 Lapham Street El Segundo, California ATTN: Mr. E. H. Heineman, Chief Engineer Antenna Group Electrical Section	1
I 249	Boeing Airplane Company Pilotless Aircraft Division Post Office Box 3707 Seattle 24, Washington ATTN: R. R. Barber, Library Supervisor	2
I 279	Lockheed Aircraft Corporation California Division Engineering Library 2555 N. Hollywood Way Dept. 72-25, Plant A-1, Bldg. 63-1 Burbank, California ATTN: N. C. Harnois	1
I 282	Radio Corporation of America Laboratories David Sarnoff Research Center Princeton, New Jersey ATTN: Miss Fern Cloak, Librarian, Research Library	1
U 32	Massachusetts Institute of Technology Research Laboratory of Electronics Document Room 20B-221 Cambridge 39, Mass.	1
U 158	Massachusetts Institute of Technology Lincoln Laboratory Post Office Box 73 Lexington 73, Mass. ATTN: Henry Straus, Document Room A-229	1
U 79	University of Michigan Engineering Research Institute Radiation Laboratory, 912 N. Main St. Ann Arbor, Michigan via: Facility Security Officer ATTN: Prof. K. M. Siegel	1
U 48	Polytechnic Institute of Brooklyn Microwave Research Institute 55 Johnson Street Brooklyn 1, New York ATTN: Dr. A. A. Oliner	1
U 146	University of Tennessee Ferris Hall West Cumberland Avenue Knoxville, Tennessee ATTN: Prof. J. D. Tillman, Jr.	1
U 100	Electronics Research Laboratory University of California 332 Cory Hall Berkeley 4, California ATTN: J. R. Whinnery, Prof.	1
U 99	California Institute of Technology 1201 E. California Street Pasadena, California ATTN: Dr. Charles H. Papas	1
U 10	Cornell University School of Electrical Engineering Ithaca, New York ATTN. Prof. G. C. Dalman	1
U 59	Library Georgia Institute of Technology Engineering Experiment Station Atlanta, Georgia ATTN: Mrs. J. H. Crosland, Librarian	1
U 102	Harvard University Technical Reports Collection Gordon McKay Library, 303A Pierce Hall Oxford Street Cambridge 38, Mass. ATTN: Mrs. E. L. Hufschmidt, Librarian	1

DISTRIBUTION LIST

Code	Organization	No. of Copies
N 23	U. S. Naval Ordnance Laboratory White Oak Silver Spring 19, Maryland ATTN: The Library	1
N 26	Commander U. S. Naval Ordnance Test Station China Lake, California ATTN: Code 753	1
N 27	Librarian U. S. Naval Postgraduate School Monterey, California	1
N 28	Air Force Development Field Representative Naval Research Laboratory Washington 25, D. C. ATTN: Code 1072	1
N 29	Director U. S. Naval Research Laboratory Washington 25, D. C. ATTN: Code 2027	1
N 30	Dr. J. I. Bohnert, Code 5210 U. S. Naval Research Laboratory Washington 25, D. C.	1
N 35	Commanding Officer and Director U. S. Navy Underwater Sound Laboratory Fort Trumbull, New London, Connecticut	1
N 37	Chief of Naval Research Department of the Navy Washington 25, D. C. ATTN: Code 427	1
N 85	Commanding Officer and Director U. S. Navy Electronics Laboratory (Library) San Diego 52, California	2
N 9	Chief, Bureau of Ordnance Department of the Navy Washington 25, D. C. ATTN: Code Ad3	1
N 86	Chief, Bureau of Ordnance Department of the Navy Surface Guided Missile Branch Washington 25, D. C. ATTN: Code ReS1-e	1
N 87	Chief, Bureau of Ordnance Department of the Navy Washington 25, D. C. ATTN: Fire Control Branch (ReS4)	1
N 88	Department of the Navy Bureau of Aeronautics Technical Data Division Code 4106 Washington 25, D. C.	1
N 48	Commanding Officer U. S. Naval Air Development Center Johnsonville, Pennsylvania ATTN: NADC Library	2
N 91	Commander U. S. Naval Air Test Center Patuxent River, Maryland ATTN: ET-315, Antenna Branch	1
N 92	New York Naval Shipyard Material Laboratory, Code 932 Brooklyn 1, New York ATTN: Mr. Douglas First	1
N 93	Director Naval Ordnance Laboratory Corona, California	1
N 97	Commanding Officer U. S. Naval Ordnance Laboratory Corona, California ATTN: Mr. W. Horenstein, Division 72	1
I 205	Battelle Memorial Institute 505 King Avenue Columbus 1, Ohio ATTN: Wayne E. Rife, Project Leader, Electrical Engineering Division	1
I 3	Andrew Alford Consulting Engineers 299 Atlantic Avenue Boston 10, Mass.	1
I 260	Sylvania Elec. Products, Inc. Electronic Defense Laboratory P. O. Box 205 Mountain View, California ATTN: Library	1
I 269	General Electric Company Electronics Park Syracuse, New York ATTN: Bessie Fletcher, Documents Library, Building 3-143A	1
I 207	Hughes Aircraft Company Antenna Department Microwave Laboratory, Bldg. 12, Room 2617 Culver City, California ATTN: M. D. Adcock	1
I 232	Radiation Engineering Laboratory Main Street Maynard, Massachusetts ATTN: Dr. John Ruze	1
I 23[illegible]	Raytheon Manufacturing Company Wayland Laboratory State Road Wayland, Massachusetts ATTN: Mr. [illegible]bert Borts	1
I 25[illegible]	Stanford Research Institute Menlo Park, California ATTN: Library, Engineering Division	1
I 144	Maryland Electronic Manufacturing Corp. 5009 Calvert Road College Park, Maryland ATTN: Mr. H. Warren Cooper	1
I 66	The W. L. Maxson Corporation 460 West 34th Street New York, New York ATTN: Miss Dorothy Clark	1
I 284	North American Aviation, Inc. 12214 Lakewood Boulevard Downey, California ATTN: Engineering Library 495-115	1
I 289	Radiation, Inc. P. O. Drawer 37 Melbourne, Florida ATTN: Technical Library, Mr. M. L. Cox	1
I 233	Radio Corporation of America RCA Laboratories Rocky Point, New York ATTN: P. S. Carter, Lab. Library	1
I 312	The Ramo-Wooldridge Corporation Post Office Box 45453 Airport Station Los Angeles 45, California ATTN: Margaret C. Whitnah, Chief Librarian	2
I 149	Raytheon Manufacturing Company Missile Systems Division Bedford, Mass. ATTN: Mr. Irving Goldstein	1
I 142	Sanders Associates, Inc. 95 Canal Street Nashua, New Hampshire ATTN: N. R. Wild, Library	1
I 297	Sperry Gyroscope Company Great Neck, Long Island, New York ATTN: Florence W. Turnbull, Engr. Librarian	1
I 104	Sylvania Electric Products, Inc. 100 First Avenue Waltham 54, Mass. ATTN: Charles A. Thornhill, Reports Librarian Waltham Laboratories Library	1
G 6	Library Boulder Laboratories National Bureau of Standards Boulder, Colorado	1

DISTRIBUTION LIST

Code	Organization	No. of Copies
U 104	University of Illinois College of Engineering Urbana, Illinois ATTN: Dr. P. E. Mayes, Dept. of Electrical Engineering	1
U 22	The Johns Hopkins University Homewood Campus Department of Physics Baltimore 18, Maryland ATTN: Dr. Donald E. Kerr	1
U 78	Ohio State University Research Foundation Columbus 10, Ohio ATTN: Dr. T. E. Tice, Dept. of Electrical Engineering	1
U 110	Syracuse University Research Institute Collendale Campus Syracuse 10, New York ATTN: Dr. C. S. Grove, Jr., Director of Engineering Research	1
U 51	The University of Texas Defense Research Laboratory Austin 12, Texas ATTN: Claude W. Horton, Physics Library	1
U 133	University of Washington Department of Electrical Engineering Seattle 5, Washington ATTN: G. Held, Associate Professor	1
I 116	Melpar, Inc. 3000 Arlington Boulevard Falls Church, Virginia ATTN: Engineering Technical Library	1

UNCLASSIFIED

UNCLASSIFIED